

Set-Based Training for Neural Network Verification

Lukas Koller, Tobias Ladner, and Matthias Althoff

Abstract—Neural networks are vulnerable to adversarial attacks, i.e., small input perturbations can significantly affect the outputs of a neural network. Therefore, to ensure safety of safety-critical environments, the robustness of a neural network must be formally verified against input perturbations, e.g., from noisy sensors. To improve the robustness of neural networks and thus simplify the formal verification, we present a novel set-based training procedure in which we compute the set of possible outputs given the set of possible inputs and compute for the first time a gradient set, i.e., each possible output has a different gradient. Therefore, we can directly reduce the size of the output enclosure by choosing gradients toward its center. Small output enclosures increase the robustness of a neural network and, at the same time, simplify its formal verification. The latter benefit is due to the fact that a larger size of propagated sets increases the conservatism of most verification methods. Our extensive evaluation demonstrates that set-based training produces robust neural networks with competitive performance, which can be verified using fast (polynomial-time) verification algorithms due to the reduced output set.

Index Terms—Neural network verification, set-based computing, adversarial robustness, and adversarial training.

I. INTRODUCTION

Neural networks demonstrate impressive performance for many complex tasks, such as speech recognition [1] or object detection [2]. However, many neural networks are sensitive to input perturbations [3]: Small, carefully chosen input perturbations can lead to vastly different outputs. This behavior is problematic for the adoption of neural networks in safety-critical environments, where the input often contains noisy sensor data or is subject to external disturbances, e.g., autonomous vehicle control [4] or airborne collision avoidance [5]. Thus, the formal verification of neural networks gained interest in recent years [6]. Given a set of inputs, the formal verification of neural networks attempts to find a proof that the neural network returns the correct output for every input from the set. Typically, when verifying the robustness of a neural network, the perturbations are modeled as an ℓ_∞ -ball of radius $\epsilon \in \mathbb{R}_{>0}$ around an input.

In this work, we address the challenge of training and verifying the robustness of a neural network with a novel set-based training procedure. During training, we enclose the output set of the neural network and compute a gradient set, i.e., each possible output has a different gradient. We can directly enforce smaller output enclosures by choosing gradients that point toward the center of the enclosure. To compute the gradient set, we use a set-based loss function, which considers the position (for accuracy) and the size of the output enclosure (for robustness). Small output enclosures improve the robustness of the neural network and simplify subsequent formal verification. Previous works are limited to

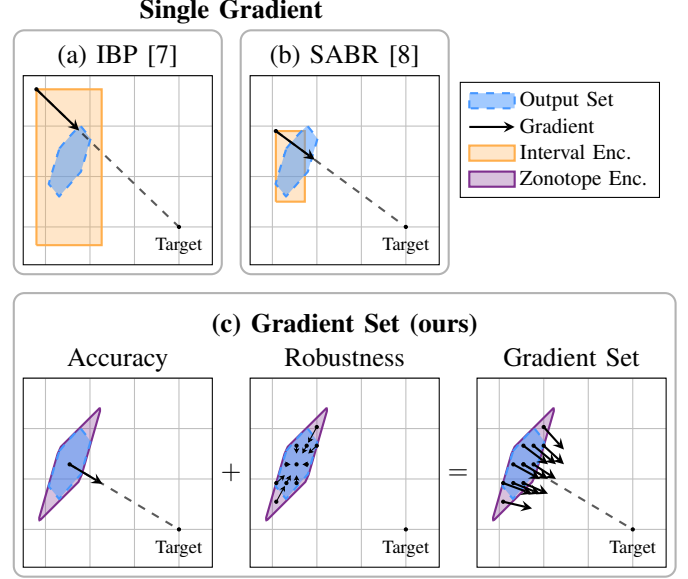


Fig. 1. Comparing our gradient set with the gradient of other robust training approaches for the same neural network in the output space. The blue area shows the exact output set of the neural network. Other training approaches ((a) IBP and (b) SABR) propagate intervals to compute a single gradient. On the contrary, our set-based training (c) computes a gradient set based on the position (for accuracy) and size (for robustness) of the output set.

a single gradient for training, thereby discarding much set-based information. Fig. 1 compares our gradient set with the gradient of two robust training approaches: Interval bound propagation (IBP) [7] and SABR [8]. IBP computes bounds of the output set and uses the gradient of the worst-case output; SABR uses the gradient of the worst case of a smaller input region to reduce regularization by large approximation errors. Subsequently, we provide an overview of related work.

A. Formal Verification of Neural Networks

The formal verification of neural networks is computationally challenging, i.e., the problem is NP-hard with only rectified linear unit (ReLU) activation functions [9]; thus, even verifying small neural networks often takes a long time. Most formal verification approaches either formulate an optimization problem, which is solved with an off-the-shelf solver, e.g., (mixed-integer) linear programming [10], [11] or satisfiability modulo theories (SMT) [9], or use reachability analysis [6]. Often, branch-and-bound algorithms [12], [13] are utilized for the verification of neural networks: The input space is recursively split until each subspace of the input space is either verified or falsified; due to the recursive process, branch-and-bound algorithms have exponential runtime in the worst case. Hence, many verification methods sacrifice accuracy for a polynomial runtime: Reachability analysis uses efficient set

representations, e.g., zonotopes [14], combined with set-based computations to efficiently enclose the output set of a neural network (in polynomial time) [15]–[18]. If the enclosure of the output set is sufficiently tight, it can be used to formally verify a neural network.

On the contrary, neural networks can be falsified by adversarial attacks, i.e., small input perturbations that lead to an incorrect output. Often, adversarial attacks are fast to compute and effective at provoking incorrect outputs [19]. The most prominent approaches are the fast gradient sign method (FGSM) and projected gradient descent (PGD). The FGSM is a single-step gradient-based adversarial attack that efficiently generates adversarial attacks [19]. PGD uses multiple iterations of FGSM to compute stronger adversarial attacks [20]. However, neural networks can be robust for one type of attack but can remain vulnerable to another type of attack [21]; thus, it is necessary to formally verify the robustness of neural networks.

B. Training Robust Neural Networks

The training objective of a robust neural network is typically formulated as a min-max optimization problem [21]: minimize the worst-case loss within a set of input possible inputs. Computing the worst-case loss within a set is computationally difficult [22]. Nonetheless, robust neural networks can be effectively trained by approximating the worst-case loss with adversarial attacks, e.g., computed using PGD [21].

The well-established trade-off loss [23] combines a regular loss for accuracy with a boundary loss for robustness, which is approximated with adversarial attacks. The boundary loss pushes the decision boundary of a classifier away from the training samples and thereby improves the robustness of the trained neural network. However, neural networks trained with adversarial attacks remain hard to formally verify.

Therefore, some approaches combine the training and formal verification of neural networks. In these works, the approximation of a worst-case loss is replaced by an upper bound, guaranteeing that no perturbation will lead to an incorrect output. Different methods for computing an upper bound of the worst-case loss have been proposed: Interval bound propagation (IBP) [7], linear relaxation [24], (mixed-integer) linear programming [25], or abstract interpretation [26]. IBP computes conservative output bounds and uses the worst case within the bounds for training and verification [7] (Fig. 1a). Large approximation errors can create an over-regularization and lead to poor performance [8].

Thus, by propagating smaller input sets, state-of-the-art robustness results are achieved [8] (Fig. 1b). However, a branch-and-bound algorithm with worst-case exponential-time complexity is used for their formal verification. Instead, we aim to train neural networks that can be quickly verified using polynomial-time verification algorithms. Moreover, IBP can be combined with adversarial attacks computed in a latent space [27]. Similarly, zonotopes can be partially propagated through a neural network to compute adversarial attacks in latent space [28]; however, the partial propagation results in layer-wise training of the neural network, which has a significant computational overhead. Furthermore, the training of

robust neural networks can be improved by using a specialized initialization for the parameters of a neural network [29].

More closely related to our work is an approach using zonotopic enclosures during training [26]; however, much set-based information is discarded by only using the enclosure to bound the worst-case loss. All related approaches for training robust neural networks consider a single gradient. Conversely, our approach considers a gradient set (Fig. 1c), thereby simultaneously increasing the robustness of the neural network and simplifying the formal verification.

C. Contributions

Our main contributions are:

- A novel set-based training procedure for robust neural networks that, for the first time, uses a gradient set for training that generalizes the well-established trade-off loss [23]. The gradient set enables direct control of the size of the output enclosure to improve the robustness of the neural network and simplify formal verification.
- A fast, batch-wise, and differentiable set-based forward propagation and backpropagation that is efficiently computed on a GPU. The set propagation uses analytical solutions for the image enclosure of typical nonlinear activation functions.
- An extensive empirical evaluation in which we demonstrate the competitive performance of our set-based training and compare it with state-of-the-art robust training approaches. Moreover, we include large-scale ablation studies to justify our design choices.

D. Organization

We introduce the required preliminaries in Sec. II. In Sec. III, we present our set-based training procedure, which benefits from a fast, batch-wise, and differentiable set propagation derived in Sec. IV. We provide an empirical evaluation, including ablation studies in Sec. V. Finally, we conclude our findings in Sec. VI.

II. PRELIMINARIES

A. Notation

Lowercase letters denote vectors and uppercase letters denote matrices. The i -th entry of a vector x is denoted by $x_{(i)}$. For a matrix $A \in \mathbb{R}^{n \times m}$, $A_{(i,j)}$ denotes the entry in the i -th row and the j -th column, $A_{(i,\cdot)}$ denotes the i -th row, and $A_{(\cdot,j)}$ the j -th column. The identity matrix is written as $I_n \in \mathbb{R}^{n \times n}$. We use $\mathbf{0}$ and $\mathbf{1}$ to represent the vector or matrix (with appropriate size) that contains only zeros or ones. Given two matrices $A \in \mathbb{R}^{m \times n_1}$ and $B \in \mathbb{R}^{m \times n_2}$, their (horizontal) concatenation is denoted by $[A \ B] \in \mathbb{R}^{m \times (n_1+n_2)}$; if $n_1 = n_2$, their Hadamard product is the element-wise multiplication $(A \odot B)_{(i,j)} = A_{(i,j)} B_{(i,j)}$. The operation $\text{Diag}: \mathbb{R}^n \rightarrow \mathbb{R}^{n \times n}$ returns a diagonal matrix with the entries of a given vector on its diagonal. We denote sets with uppercase calligraphic letters. For a set $\mathcal{S} \subset \mathbb{R}^n$, we denote its projection to the i -th dimension by $\mathcal{S}_{(i)}$. Given two sets $\mathcal{S}_1 \subset \mathbb{R}^n$ and $\mathcal{S}_2 \subset \mathbb{R}^m$, we denote the Cartesian product by $\mathcal{S}_1 \times \mathcal{S}_2 = \{[s_1^\top \ s_2^\top]^\top \mid$

$s_1 \in \mathcal{S}_1, s_2 \in \mathcal{S}_2\}$, and if $n = m$, we write the Minkowski sum as $\mathcal{S}_1 \oplus \mathcal{S}_2 = \{s_1 + s_2 \mid s_1 \in \mathcal{S}_1, s_2 \in \mathcal{S}_2\}$. For $n \in \mathbb{N}$, $[n] = \{1, 2, \dots, n\}$ denotes the set of all natural numbers up to n . An n -dimensional interval $\mathcal{I} \subset \mathbb{R}^n$ with bounds $l, u \in \mathbb{R}^n$ is denoted by $\mathcal{I} = [l, u]$, where $\forall i \in [n]: l_{(i)} \leq u_{(i)}$. For a function $f: \mathbb{R}^n \rightarrow \mathbb{R}^m$, we abbreviate its evaluation for a set $\mathcal{S} \subset \mathbb{R}^n$ with $f(\mathcal{S}) = \{f(s) \mid s \in \mathcal{S}\}$. The derivative of a scalar function $f: \mathbb{R} \rightarrow \mathbb{R}$ is denoted as $f'(x) = \mathrm{d}/\mathrm{d}x f(x)$. Moreover, the gradient of a function $f: \mathbb{R}^n \rightarrow \mathbb{R}$ w.r.t. a vector $x \in \mathbb{R}^n$ is its element-wise derivative: $(\nabla_x f(x))_{(i)} = \partial/\partial x_{(i)} f(x)$, for $i \in [n]$. Analogously, we define the gradient of a function $f: \mathbb{R}^{n \times m} \rightarrow \mathbb{R}$ w.r.t. a matrix $A \in \mathbb{R}^{n \times m}$: $(\nabla_A f(A))_{(i,j)} = \partial/\partial A_{(i,j)} f(A)$, for $i \in [n]$ and $j \in [m]$.

B. Feed-Forward Neural Networks

A feed-forward neural network $N_\theta: \mathbb{R}^{n_0} \rightarrow \mathbb{R}^{n_\kappa}$ consists of a sequence of $\kappa \in \mathbb{N}$ layers. For the k -th layer, $n_{k-1} \in \mathbb{N}$ denotes the number of input neurons and $n_k \in \mathbb{N}$ denotes the number of output neurons. A layer can either be a linear layer, which applies an affine map, or a nonlinear (activation) layer, which applies a nonlinear activation function element-wise.

Definition 1 (Neural Network, [30, Sec. 5.1]). *For an input $x \in \mathbb{R}^{n_0}$, the output $y = N_\theta(x) \in \mathbb{R}^{n_\kappa}$ of a neural network N_θ is computed by*

$$h_0 = x, \quad h_k = L_k(h_{k-1}) \quad \text{for } k \in [\kappa], \quad y = h_\kappa,$$

where

$$h_k = L_k(h_{k-1}) = \begin{cases} W_k h_{k-1} + b_k & \text{if } k\text{-th layer is linear,} \\ \phi_k(h_{k-1}) & \text{otherwise,} \end{cases}$$

with weights $W_k \in \mathbb{R}^{n_k \times n_{k-1}}$, bias $b_k \in \mathbb{R}^{n_k}$, and nonlinear activation function ϕ_k which is applied element-wise.

We denote the parameters of the neural network with θ , which include all weight matrices and bias vectors from its linear layers.

a) Training of Neural Networks: We consider supervised training settings of a classification task, where a neural network is trained on a dataset $\mathcal{D} = \{(x_1, t_1), \dots, (x_n, t_n)\}$, containing inputs $x_i \in \mathbb{R}^{n_0}$ with associated targets $t_i \in \{0, 1\}^{n_\kappa}$. A target $t_i \in \{0, 1\}^{n_\kappa}$ is a one-hot encoding of the target label $l_i \in [n_\kappa]$, i.e., $t_i = e_{l_i}$ is the l_i -th standard basis vector e_{l_i} . A loss function $L: \mathbb{R}^{n_\kappa} \times \mathbb{R}^{n_\kappa} \rightarrow \mathbb{R}$ measures how well a neural network predicts the targets. A typical loss function for classification tasks is the cross-entropy error:

$$L_{\text{CE}}(t, y) := - \sum_{i=1}^{n_\kappa} t_{(i)} \ln(p_{(i)}), \quad (1)$$

where \ln denotes the natural logarithm and $p_{(i)} = \exp(y_{(i)})/(\exp(y) \mathbf{1})$ are the predicted class probabilities. The training goal of a neural network is to find parameters θ that minimize the total loss of the dataset \mathcal{D} [30, Sec. 5.2]:

$$\min_{\theta} \sum_{(x_i, t_i) \in \mathcal{D}} L(t_i, N_\theta(x_i)). \quad (2)$$

We revisit the training of a neural network to later augment it with sets. A popular algorithm to train a neural network is

gradient descent [30, Sec. 5.2.4]: the parameters are randomly initialized [31] and iteratively optimized using the gradient of the loss function. We denote the gradient of the loss function L w.r.t. the output of the k -th layer h_k as:

$$g_k := \nabla_{h_k} L(t, y), \quad (3)$$

where $y = N_\theta(x)$ for input $x \in \mathbb{R}^{n_0}$. The weight matrix W_k and bias vector b_k of the k -th layer are updated as [30, Sec. 5.3]

$$\begin{aligned} W_k &\leftarrow W_k - \eta \nabla_{W_k} L(t, y) = W_k - \eta g_k h_{k-1}^\top, \\ b_k &\leftarrow b_k - \eta \nabla_{b_k} L(t, y) = b_k - \eta g_k, \end{aligned} \quad (4)$$

where $\eta \in \mathbb{R}_{>0}$ is the learning rate. The gradients g_k are efficiently computed with backpropagation [30, Sec. 5.3]: by utilizing the chain rule, the gradient g_κ of the last layer is propagated backward through all neural network layers.

Proposition 1 (Backpropagation, [30, Sec. 5.3]). *Let $y \in \mathbb{R}^{n_\kappa}$ be an output of a neural network with target $t \in \mathbb{R}^{n_\kappa}$. The gradients g_k are computed in reverse order as*

$$\begin{aligned} g_\kappa &= \nabla_y L(t, y), \\ g_{k-1} &= \begin{cases} W_k^\top g_k & \text{if } k\text{-th layer is linear,} \\ \text{Diag}(\phi'_k(h_{k-1})) g_k & \text{otherwise,} \end{cases} \end{aligned}$$

for all $k \in \{\kappa, \dots, 1\}$.

From now on, we refer to this (standard) neural network training as point-based training.

C. Set-Based Computation

Our approach extends point-based training to sets, which we represent by zonotopes. A zonotope is a convex set representation describing the Minkowski sum of a finite number of line segments.

Definition 2 (Zonotope, [14, Def. 1]). *Given a center $c \in \mathbb{R}^n$ and a generator matrix $G \in \mathbb{R}^{n \times q}$, a zonotope $\mathcal{Z} \subset \mathbb{R}^n$ is defined as*

$$\mathcal{Z} = \{c + G\beta \mid \beta \in [-1, 1]^q\} =: \langle c, G \rangle_{\mathcal{Z}}.$$

Subsequently, we define several operations for zonotopes used in our training approach. Please note, that for the complexity analysis, we only consider the number of binary operations and we neglect the computational effort of unary operations. Moreover, we consider the textbook method and do not assume any special numerical tricks that have been developed for large matrices.

Proposition 2 (Interval Enclosure, [32, Prop. 2.2]). *A zonotope $\mathcal{Z} = \langle c, G \rangle_{\mathcal{Z}}$ with $c \in \mathbb{R}^n$ and $G \in \mathbb{R}^{n \times q}$ is enclosed by the interval $[l, u] \supseteq \mathcal{Z}$, where*

$$l = c - |G| \mathbf{1}, \quad u = c + |G| \mathbf{1},$$

and $|\cdot|$ computes the element-wise absolute value. The time complexity of computing an interval enclosure is $\mathcal{O}(nq)$.

Proposition 3 (Minkowski Sum, [32, Prop. 2.1 and Sec. 2.4]). *The Minkowski sum of a zonotope $\mathcal{Z} = \langle c, G \rangle_{\mathcal{Z}}$ and an*

interval $\mathcal{I} = [l, u] \subset \mathbb{R}^n$ with $c, l, u \in \mathbb{R}^n$ and $G \in \mathbb{R}^{n \times q}$ is computed as

$$\mathcal{Z} \oplus \mathcal{I} = \langle c + 1/2(u + l), [G \quad 1/2 \text{Diag}(u - l)] \rangle_{\mathcal{Z}},$$

and has time complexity $\mathcal{O}(n)$.

Proposition 4 (Affine Map, [32, Sec. 2.4]). *The result of an affine map $f: \mathbb{R}^n \rightarrow \mathbb{R}^m$, $x \mapsto Wx + b$ with $W \in \mathbb{R}^{m \times n}$ and $b \in \mathbb{R}^m$ applied to a zonotope $\mathcal{Z} = \langle c, G \rangle_{\mathcal{Z}}$ with $c \in \mathbb{R}^n$ and $G \in \mathbb{R}^{n \times q}$ is*

$$f(\mathcal{Z}) = \{f(z) \mid z \in \mathcal{Z}\} = W\mathcal{Z} + b = \langle Wc + b, WG \rangle_{\mathcal{Z}},$$

and has time complexity $\mathcal{O}(mnq)$.

Determining the volume of a zonotope is computationally demanding [33]. However, we can effectively approximate the size of a zonotope with its F-radius [34]: The F-radius of a zonotope is the Frobenius norm of its generator matrix.

Proposition 5 (F-Radius, [34, Def. 3]). *For a zonotope $\mathcal{Z} = \langle c, G \rangle_{\mathcal{Z}} \subset \mathbb{R}^n$ with $G \in \mathbb{R}^{n \times q}$, the F-radius is*

$$\|\mathcal{Z}\|_F := 1/n \sqrt{\sum_{i=1}^n \sum_{j=1}^q G_{(i,j)}^2}.$$

Please note that in contrast to [34, Def. 3], we include a normalization factor of $1/n$. For set-based training, we require the gradient of a function w.r.t. a zonotope, which is also a zonotope, where the center is the derivative w.r.t. the center and the generator matrix is the derivative w.r.t. the generator matrix.

Definition 3 (Zonotope Gradient). *The gradient of a function $f(\cdot)$ w.r.t. a zonotope $\mathcal{Z} = \langle c, G \rangle_{\mathcal{Z}} \subset \mathbb{R}^n$ is defined as*

$$\nabla_{\mathcal{Z}} f(\mathcal{Z}) := \langle \nabla_c f(\mathcal{Z}), \nabla_G f(\mathcal{Z}) \rangle_{\mathcal{Z}}.$$

D. Formal Verification of Neural Networks

In this work, we consider the robustness of neural networks for classification tasks: Each dimension of an output $y \in \mathbb{R}^{n_\kappa}$ corresponds to a class, and the dimension with the maximum value determines the predicted class. An input $x \in \mathbb{R}^{n_0}$ is correctly classified by a neural network if the predicted class matches the target label:

$$\arg \max_{k \in [n_\kappa]} y_{(k)} = l. \quad (5)$$

We call a neural network (locally) robust for a given set of inputs if the neural network correctly classifies every input within the set. As an input set, we use the ℓ_∞ -ball of radius $\epsilon \in \mathbb{R}_{>0}$ around an input $x \in \mathbb{R}^{n_0}$:

$$\pi_\epsilon(x) := \langle x, \epsilon I_{n_0} \rangle_{\mathcal{Z}} = \{ \tilde{x} \in \mathbb{R}^{n_0} \mid \|\tilde{x} - x\|_\infty \leq \epsilon \}. \quad (6)$$

For an input set $\mathcal{X} = \pi_\epsilon(x) \subset \mathbb{R}^{n_0}$, we formally verify the robustness of a neural network N_θ by using set-based computations to efficiently compute (in polynomial time) an enclosure $\mathcal{Y} \subset \mathbb{R}^{n_\kappa}$ of its output set $\mathcal{Y}^* := N_\theta(\mathcal{X}) \subseteq \mathcal{Y}$. If \mathcal{Y} does not contain unsafe outputs, we have formally verified the neural network for the input set \mathcal{X} . Fig. 2 illustrates the formal verification of a neural network. For a classification

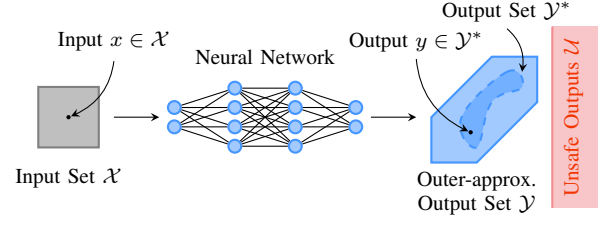


Fig. 2. Verifying the local robustness of a neural network.

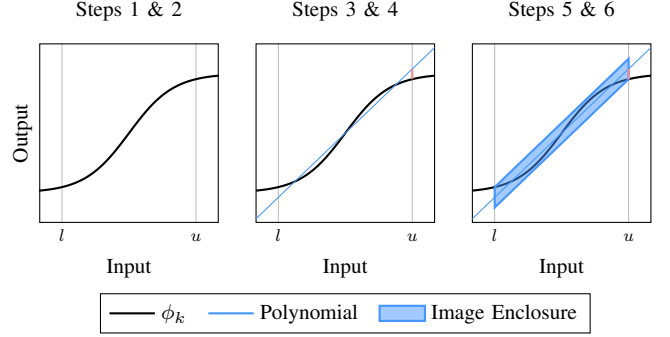


Fig. 3. Main steps of an image enclosure [18, Prop. 2.14].

task with target label $l \in \mathbb{R}^{n_\kappa}$, the unsafe set contains every incorrect classification [18, Prop. B.2], i.e., there is a dimension $k \in [n_\kappa]$ for which the output $y_{(k)}$ is larger than the output of the target dimension $y_{(l)}$:

$$\mathcal{U}_t := \{y \in \mathbb{R}^{n_\kappa} \mid \exists k \in [n_\kappa]: y_{(k)} > y_{(l)}\}. \quad (7)$$

To compute an enclosure \mathcal{Y} , we evaluate the layers (Def. 1) over sets. The output set of a linear layer is computed with an affine map [18, Sec. 2.4]; whereas, the output set of a nonlinear layer is enclosed as it cannot be computed exactly for zonotopes, i.e., zonotopes are not closed under nonlinear maps. The required steps are summarized in Fig. 3. The activation function is applied element-wise; hence, the input dimensions are considered independently. We first project the input set onto a dimension and compute bounds (Steps 1 & 2). The activation function is approximated using a linear polynomial, and to ensure the soundness, a bound on the approximation errors is computed (Steps 3 & 4). Finally, the approximation is evaluated over the input set, and the approximation errors are added (Steps 5 & 6).

We define the following set-based forward propagation.

Proposition 6 (Set-Based Forward Prop., [18, Sec. 2.4]). *For an input set $\mathcal{X} \subset \mathbb{R}^{n_0}$, an enclosure $\mathcal{Y} \subset \mathbb{R}^{n_\kappa}$ of the output set $\mathcal{Y}^* := N_\theta(\mathcal{X})$ of a neural network can be computed as*

$$\begin{aligned} \mathcal{H}_0 &= \mathcal{X}, \\ \mathcal{H}_k &= \begin{cases} W_k \mathcal{H}_{k-1} + b_k & \text{if } k\text{-th layer is linear,} \\ \text{enclose}(\phi_k, \mathcal{H}_{k-1}) & \text{otherwise,} \end{cases} \\ &\quad \text{for } k \in [\kappa], \\ \mathcal{Y} &= \mathcal{H}_\kappa. \end{aligned}$$

The operation `enclose` computes an image enclosure of a nonlinear layer, e.g. [18, Prop. 2.14].

The enclosure of the output set of a neural network N_θ is denoted by $\mathcal{Y} = \text{enclose}(N_\theta, \mathcal{X})$.

E. Problem Statement

We want to leverage set-based training to create robust neural networks.

Definition 4 (Set-Based Training). *Given a set-based loss function $\mathcal{L} : \mathbb{R}^{n_\kappa} \times 2^{\mathbb{R}^{n_\kappa}} \rightarrow \mathbb{R}$, set-based training trains a neural network using a gradient set $\nabla_{\mathcal{Y}} \mathcal{L}(t, \mathcal{Y}) \subset \mathbb{R}^{n_\kappa}$ (Def. 3), which defines a different gradient $g \in \nabla_{\mathcal{Y}} \mathcal{L}(t, \mathcal{Y})$ for each point $y \in \mathcal{Y}$.*

Set-based training can directly enforce smaller output sets by choosing gradients that point toward the center of an output set (Fig. 4). Thereby, we can simultaneously improve the robustness of the neural network and simplify the formal verification. Therefore, we want to use set-based training to train the parameters θ of a robust neural network N_θ :

$$\min_{\theta} \sum_{(x_i, t_i) \in \mathcal{D}} \mathcal{L}(t_i, \text{enclose}(N_\theta, \pi_\epsilon(x_i))).$$

By reducing the size of the output set using set-based training, we can verify neural networks with fast (polynomial time) algorithms.

III. SET-BASED TRAINING OF NEURAL NETWORKS

We present a novel set-based algorithm to train robust neural networks with a gradient set (Def. 4). In each training iteration, we (i) enclose the output set of the neural network by zonotopes (Sec. IV-A), (ii) compute a gradient set derived from a set-based loss function using features of the output enclosure (Sec. III-A), (iii) backpropagate the gradient set (Sec. IV-B), and (iv) aggregate over the gradient set to update the parameters of the neural network (Sec. IV-C).

A. Set-Based Loss Function and Gradient Set

We derive the gradient set used for training by computing the gradient of a set-based loss function which maps an output set to a loss value (Def. 4). In this work, we define the set-based loss function $\mathcal{L} : \mathbb{R}^{n_\kappa} \times 2^{\mathbb{R}^{n_\kappa}} \rightarrow \mathbb{R}$ so that it combines (i) a standard loss of the center of the enclosure (for accuracy) with (ii) the F-radius (Prop. 5) of the enclosure to approximate its size (for robustness) (Fig. 1c).

Definition 5 (Set-Based Loss). *Given a loss function $L : \mathbb{R}^{n_\kappa} \times \mathbb{R}^{n_\kappa} \rightarrow \mathbb{R}$, we define a set-based loss function as*

$$\mathcal{L}(t, \mathcal{Y}) := \underbrace{(1 - \tau) L(t, c_\kappa)}_{\text{Accuracy}} + \underbrace{\tau/\epsilon \|\mathcal{Y}\|_F}_{\text{Robustness}},$$

where $\epsilon \in \mathbb{R}_{>0}$ is the perturbation radius and $\mathcal{Y} = \langle c_\kappa, G_\kappa \rangle_Z$ is an output enclosure.

The set-based loss function balances the center loss and the F-radius using a hyperparameter $\tau \in [0, 1]$, controlling the trade-off between accuracy and robustness. To make tuning the hyperparameter τ easier, the F-radius in Def. 5 is normalized using the input perturbation radius $\epsilon \in \mathbb{R}_{>0}$. The normalization

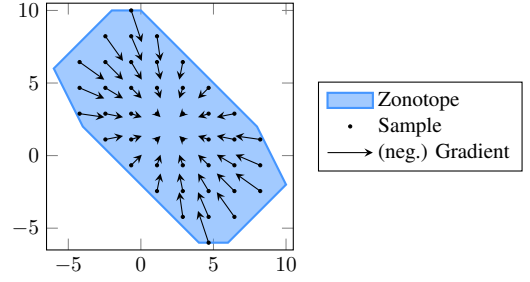


Fig. 4. Gradients of the F-radius of a zonotope.

is derived by taking the ratio of the F-radii of output enclosure \mathcal{Y} and input set $\mathcal{X} = \pi_\epsilon(x)$: $\|\mathcal{Y}\|_F / \|\pi_\epsilon(x)\|_F \stackrel{(6)}{=} 1/\epsilon \|\mathcal{Y}\|_F$.

Our set-based loss generalizes the well-established tradeoff-loss [23, Eq. 5], which combines a standard training loss (first summand) with a boundary loss (second summand):

$$L_{\text{TRADES}}(t, y) = L(t, y) + \max_{\tilde{x} \in \pi_\epsilon(x)} 1/\lambda L(y, N_\theta(\tilde{x})),$$

where $y = N_\theta(x)$ and λ is a weighting factor. The F-radius in our set-based loss captures the size of an output set in all dimensions and corresponds to the boundary loss, which only considers the size of the output set along a single direction. Moreover, through the sound set-based computations (Prop. 6), the set-based loss accurately over-approximates the size of the output set. In contrast, the boundary loss is only approximated in [23].

Given the set-based loss function (Def. 5), we compute its gradient to derive the gradient set. The second term of the set-based loss function is the F-radius of the output set, the gradient of which is computed as follows.

Proposition 7 (Gradient of F-Radius). *The gradient of the F-radius is*

$$\nabla_{\mathcal{Y}} \|\mathcal{Y}\|_F = \frac{1}{n_\kappa \|\mathcal{Y}\|_F} \langle \mathbf{0}, G_\kappa \rangle_Z,$$

where $\mathcal{Y} = \langle c_\kappa, G_\kappa \rangle_Z \subset \mathbb{R}^{n_\kappa}$.

Proof. See Appendix B. \square

The negative gradients of the F-radius of a zonotope point toward the center of the zonotope (Fig. 4); hence, minimizing the F-radius of a zonotope reduces the size of the zonotope. With Prop. 7, we compute the gradient set used for training:

Proposition 8 (Set-Based Loss Gradient). *The gradient of the set-based loss function \mathcal{L} is*

$$\nabla_{\mathcal{Y}} \mathcal{L}(t, \mathcal{Y}) = \left\langle (1 - \tau) \nabla_{c_\kappa} L(t, c_\kappa), \frac{\tau}{\epsilon n_\kappa \|\mathcal{Y}\|_F} G_\kappa \right\rangle_Z,$$

where $\mathcal{Y} = \langle c_\kappa, G_\kappa \rangle_Z \subset \mathbb{R}^{n_\kappa}$.

Proof. See Appendix B. \square

Fig. 1c visualizes the gradient set for samples from the output set. For effective set-based training using the gradient set, we require an efficient and differentiable set propagation, which we address next.

IV. FAST, BATCH-WISE, AND DIFFERENTIABLE SET-PROPAGATION

We require efficient, batch-wise, and differentiable set propagation for the implementation of set-based training. In this section, we first define a forward propagation with the required properties (Sec. IV-A) before we derive the corresponding set-based backpropagation (Sec. IV-B) and weight updates (Sec. IV-C). Finally, we investigate the time complexity of our set-based training (Sec. IV-D)

A. Forward Propagation

The set propagation through linear layers is computed with an affine map, which can be efficiently implemented batch-wise using matrix multiplications on a GPU. Further, we want to efficiently compute batch-wise image enclosures of nonlinear layers. Sampling-based methods [17], [18], are impractical for this task, because they use polynomial regression and thus are not efficient enough and cannot be used for backpropagation. In contrast, [16] derives fast analytical solutions for the approximation errors of a specific linear approximation of s-shaped activation functions; however, this approach causes large approximation errors. During training, large approximation errors induce an over-regularization and therefore lead to poor performance [8]. To address this issue, we derive analytical solutions for the approximation errors of an arbitrary monotonically increasing linear approximation for three typical activation functions: rectified linear unit (ReLU), hyperbolic tangent, and logistic sigmoid. Secondly, we provide a linear approximation whose approximation errors are smaller or equal to Singh's enclosure [16, Thm. 3.2] while being equally fast to compute.

For the remainder of this section, let $\phi: \mathbb{R} \rightarrow \mathbb{R}$ be a monotonically increasing function, which is approximated by a linear function $p: \mathbb{R} \rightarrow \mathbb{R}$, $x \mapsto ax + b$ within an interval $[l, u] \subset \mathbb{R}$. The approximation errors of p are given by the largest lower distance and upper distance between μ and p (Fig. 5).

Definition 6 (Approximation Error of Linear Approximation). *The approximation error of a linear approximation p for ϕ within the interval $[l, u]$ are defined as*

$$\underline{d} := \min_{x \in [l, u]} \phi(x) - p(x), \quad \bar{d} := \max_{x \in [l, u]} \phi(x) - p(x).$$

We enclose the output of the activation function ϕ as,

$$\forall x \in [l, u]: \phi(x) \in p(x) + d_c \oplus [-d, d],$$

where $d_c = 1/2 (\bar{d} + \underline{d})$ and $d = 1/2 (\bar{d} - \underline{d})$. Fig. 5 illustrates a linear approximation p of the hyperbolic tangent along with its approximation errors.

a) *Efficient Computation of Approximation Errors:* We efficiently find the approximation errors \underline{d} and \bar{d} of a linear approximation p by only checking specific points of the interval $[l, u]$.

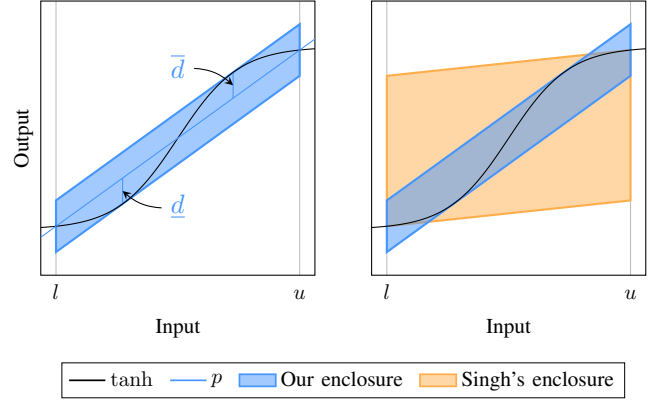


Fig. 5. Image enclosure of hyperbolic tangent: (left) Our linear approximation and approximation errors; (right) Comparison of our image enclosure and Singh's enclosure [16, Thm. 3.2].

Proposition 9 (Approximation Errors for ReLU, Hyperbolic Tangent, and Logistic Sigmoid). *The approximation error of p for $\phi \in \{\text{ReLU}, \tanh, \sigma\}$ are computed as*

$$\underline{d} = \min_{x \in \mathcal{P}_\phi \cap [l, u]} \phi(x) - p(x), \quad \bar{d} = \max_{x \in \mathcal{P}_\phi \cap [l, u]} \phi(x) - p(x),$$

where

$$\begin{aligned} \mathcal{P}_{\text{ReLU}} &= \{0, l, u\}, \\ \mathcal{P}_{\tanh} &= \{\pm \tanh^{-1}(\sqrt{1-a}), l, u\}, \text{ and} \\ \mathcal{P}_\sigma &= \{\pm 2 \tanh^{-1}(\sqrt{1-4a}), l, u\}. \end{aligned}$$

Proof. See Appendix B. \square

We note that our computation of the approximation errors works for any (monotonically increasing) linear approximation. Moreover, we observe that the offset b of the linear approximation p does not affect the image enclosure; hence, w.l.o.g. we set $b = 0$.

Definition 7 (Linear Approximation of an Activation Function). *Within the interval $[l, u]$, we approximate ϕ by a linear function $p(x) := ax$, where*

$$a := \frac{\phi(u) - \phi(l)}{u - l}.$$

Our image enclosure no longer uses a polynomial regression or requires sampling to compute the approximation errors [17, Sec. 3.2]. Moreover, only matrix multiplication and matrix addition, as well as min and max, are required. Hence, it can be efficiently computed batch-wise using matrix operations on a GPU.

b) *Our Enclosure vs. Singh's Enclosure:* We motivate the choice for our image enclosure by comparing it with Singh's enclosure [16, Thm. 3.2]. For s-shaped activation functions, e.g., hyperbolic tangent and logistic sigmoid, we prove that the approximation error of our linear approximation (Def. 7) is always smaller or equal to the approximation error of Singh's enclosure [16, Thm. 3.2] w.r.t. the area in the input-output plane (see Fig. 5) measuring the integrated approximation error over $[l, u]$:

$$\text{area}([\underline{d}, \bar{d}], [l, u]) := (u - l) (\bar{d} - \underline{d}). \quad (8)$$

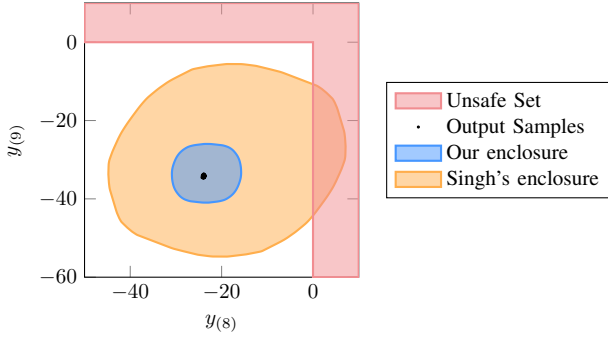


Fig. 6. Comparison of the output set of a neural network computed with our image enclosures and Singh's enclosure [16, Thm. 3.2].

Theorem 1. Let ϕ be an s -shaped function, and let $[l, u]$ be an interval. Moreover, let \underline{d} and \bar{d} be the approximation errors of p as defined in Def. 6 and 7, and let d_S be the approximation error of Singh's enclosure [16, Thm. 3.2]. It holds that

$$\text{area}([\underline{d}, \bar{d}], [l, u]) \leq \text{area}([-d_S, d_S], [l, u]).$$

Proof. See Appendix B. \square

Fig. 6 shows an instance where the output set computed with our image enclosure is significantly smaller and does not intersect the unsafe region. In contrast, the output set computed with Singh's enclosure does intersect the unsafe region.

B. Set-Based Backpropagation

We now derive the corresponding set-based backpropagation. Analogous to the point-based backpropagation (Prop. 1), the set-based backpropagation computes for every layer of the neural network the gradient set w.r.t. the output set $\mathcal{H}_k = \langle c_k, G_k \rangle_Z$:

$$\mathcal{G}_k = \langle c'_k, G'_k \rangle_Z := \nabla_{\mathcal{H}_k} \mathcal{L}(t, \mathcal{Y}). \quad (9)$$

The set-based backpropagation of linear layers is straightforward as it just applies an affine map (Prop. 1). However, the backpropagation of nonlinear layers is more involved: while the image enclosure only uses linear approximations, these depend on the input set. Thus, intuitively, we have to apply the product rule.

Proposition 10 (Backpropagation through Image Enclosure). Assume the k -th layer is a nonlinear layer with activation function ϕ_k . Given an input set $\mathcal{H}_{k-1} = \langle c_{k-1}, G_{k-1} \rangle_Z$ with $G_{k-1} \in \mathbb{R}^{n_{k-1} \times p}$ and a gradient set $\mathcal{G}_k = \langle c'_k, G'_k \rangle_Z$, the gradient set $\mathcal{G}_{k-1} = \langle c'_{k-1}, G'_{k-1} \rangle_Z$ is computed for each dimension $i \in [n_k]$ as

$$\begin{aligned} \mathcal{G}_{k-1(i)} = & \left(c'_{k(i)} c_{k-1(i)} + G'_{k(i, [p])} G_{k-1(i, \cdot)}^\top \right) \nabla_{\mathcal{H}_{k-1(i)}} a_{k(i)} \\ & + \mathcal{G}_{k(i)} a_{k(i)} + c'_{k(i)} \nabla_{\mathcal{H}_{k-1(i)}} d_{c,k(i)} \\ & + G'_{k(i, p+i)} \nabla_{\mathcal{H}_{k-1(i)}} d_{k(i)}. \end{aligned}$$

The operation `backpropEnclose` computes the gradient set of our image enclosure (Prop. 10).

Proof. See Appendix B. \square

Using the backpropagation of an image enclosure, we can (analogous to Prop. 1) backpropagate the gradient sets through all layers of a neural network.

Proposition 11 (Set-Based Backpropagation). The gradient sets \mathcal{G}_k are computed in reverse order as

$$\mathcal{G}_\kappa = \nabla_{\mathcal{Y}} \mathcal{L}(t, \mathcal{Y}),$$

$$\mathcal{G}_{k-1} = \begin{cases} W_k^\top \mathcal{G}_k & \text{if } k\text{-th layer is linear;} \\ \text{backpropEnclose}(\phi_k, \mathcal{G}_k) & \text{otherwise,} \end{cases}$$

for all $k \in \{\kappa, \dots, 1\}$.

Proof. See Appendix B. \square

C. Set-Based Update of Weights and Biases

We now describe how to use the gradient set \mathcal{G}_k and the set of inputs \mathcal{H}_{k-1} to update the weights and biases of a linear layer: Intuitively, we compute the outer product between the gradient set \mathcal{G}_k and input set \mathcal{H}_{k-1} . To avoid clutter, we define the outer product between two zonotopes $\mathcal{Z}_1 = \langle c_1, G_1 \rangle_Z \subset \mathbb{R}^{n_1}$ and $\mathcal{Z}_2 = \langle c_2, G_2 \rangle_Z \subset \mathbb{R}^{n_2}$ as

$$\mathcal{Z}_1 \odot \mathcal{Z}_2^\top := c_1 c_2^\top + G_1 G_2^\top \in \mathbb{R}^{n_1 \times n_2}. \quad (10)$$

Proposition 12 (Gradient Set w.r.t. Weights and Biases). The gradients of the set-based loss w.r.t. a weight matrix and a bias vector are

$$\begin{aligned} \nabla_{W_k} \mathcal{L}(t, \mathcal{Y}) &= \nabla_{\mathcal{H}_k} \mathcal{L}(t, \mathcal{Y}) \odot \mathcal{H}_{k-1}^\top \\ \nabla_{b_k} \mathcal{L}(t, \mathcal{Y}) &= \nabla_{\mathcal{H}_k} \mathcal{L}(t, \mathcal{Y}) \odot \langle 1, \mathbf{0} \rangle_Z^\top. \end{aligned}$$

Proof. See Appendix B. \square

The weight matrices and bias vectors are updated analogous to point-based training (4) using the gradients of the set-based loss function:

$$\begin{aligned} W_k &\leftarrow W_k - \eta \nabla_{W_k} \mathcal{L}(t, \mathcal{Y}), \\ b_k &\leftarrow b_k - \eta \nabla_{b_k} \mathcal{L}(t, \mathcal{Y}). \end{aligned} \quad (11)$$

D. Computational Complexity

Finally, we derive the time complexity of set-based training. Alg. 1 implements our image enclosure and has polynomial

Algorithm 1: Image enclosure of a nonlinear layer.

```

1 function enclose ( $\phi_k, \mathcal{H}_{k-1}$ )
2   Find bounds  $[l_{k-1}, u_{k-1}]$  of  $\mathcal{H}_{k-1}$  // Prop. 2
3   for  $i \leftarrow 1$  to  $n_k$  do
4     Find linear approx.  $a_{k(i)}$  of  $\phi_k$  // Def. 7
5     Find approx. errors  $\underline{d}_{k(i)}, \bar{d}_{k(i)}$  // Prop. 9
6      $\tilde{\mathcal{H}}_k \leftarrow \text{Diag}(a_k) \mathcal{H}_{k-1} + 1/2 (\bar{d}_k + \underline{d}_k)$  // Prop. 4
7      $\mathcal{H}_k \leftarrow \tilde{\mathcal{H}}_k \oplus [\underline{d}_k, \bar{d}_k]$  // Prop. 3
8   return  $\mathcal{H}_k$ 

```

time complexity w.r.t. the number of input dimensions and generators. Alg. 2 implements an iteration of set-based training. First, we enclose the output set of the neural network (lines 1–6). Then, we compute the gradient set \mathcal{G}_κ (line 8),

Algorithm 2: Set-based training iteration. Hyperparameters: $\epsilon \in \mathbb{R}_{>0}$, $\tau \in [0, 1]$, and $\eta \in \mathbb{R}_{>0}$.

Data: Input $x \in \mathbb{R}^{n_0}$, Target $t \in \mathbb{R}^{n_\kappa}$

Result: Neural network with updated parameters

```

1  $\mathcal{H}_0 \leftarrow \langle x, \epsilon I_{n_0} \rangle_Z$  // construct input set (6)
2 for  $k \leftarrow 1$  to  $\kappa$  do // set-based forward prop. (Prop. 6)
3   if  $k$ -th layer is linear then
4      $\mathcal{H}_k \leftarrow W_k \mathcal{H}_{k-1} + b_k$ 
5   else
6      $\mathcal{H}_k \leftarrow \text{enclose}(\phi_k, \mathcal{H}_{k-1})$ 
7  $\mathcal{Y} \leftarrow \mathcal{H}_\kappa$  // obtain output set (6)
8  $\mathcal{G}_\kappa \leftarrow \nabla_{\mathcal{Y}} \mathcal{L}(t, \mathcal{Y})$  // compute gradient set (Prop. 8)
9 for  $k \leftarrow \kappa$  to 1 do // set-based backprop. (Prop. 11)
10  if  $k$ -th layer is linear then
11     $\mathcal{G}_{k-1} \leftarrow W_k^\top \mathcal{G}_k$ 
12     $W_k \leftarrow W_k - \eta (\mathcal{G}_k \odot \mathcal{H}_{k-1}^\top)$  // Prop. 12 and (11)
13     $b_k \leftarrow b_k - \eta (\mathcal{G}_k \odot \langle 1, \mathbf{0} \rangle_Z^\top)$  // Prop. 12 and (11)
14  else
15     $\mathcal{G}_{k-1} \leftarrow \text{backpropEnclose}(\phi_k, \mathcal{G}_k)$  // Prop. 10

```

which is backpropagated through the neural network (lines 9–15). Finally, the parameters of the neural network are updated (lines 12–13).

Proposition 13 (Time Complexity of Alg. 1). *For an input set $\mathcal{H}_{k-1} = \langle c, G \rangle_Z$ with $c \in \mathbb{R}^n$ and $G \in \mathbb{R}^{n \times q}$, Alg. 1 has time complexity $\mathcal{O}(n^2 q)$ w.r.t. the number of input dimensions n and the number of generators q .*

Proof. See Appendix B. \square

Proposition 14 (Time Complexity of Alg. 2). *The zonotopes used in Alg. 2 have at most $q \leq n_0 + \sum_{k \in [\kappa]} n_k$ number of generators. Let $n_{\max} := \max_{k \in [\kappa]} n_{k-1} n_k$ be the maximum size of a weight matrix in the neural network. Moreover, Alg. 2 has time complexity $\mathcal{O}(n_{\max} q \kappa)$ w.r.t. n_{\max} , q and the number of layers κ .*

The time complexity of set-based training is polynomial, and compared to point-based training, only has an additional factor $q \in \mathcal{O}(n_0 + \sum_{k \in [\kappa]} n_k)$. The increased time complexity is expected because set-based training propagates entire generator matrices through the neural network. Moreover, for some linear relaxation methods, similar time complexities are reported [35].

V. EVALUATION

We use the MATLAB toolbox CORA [36] to implement set-based training. Following previous works [7], we train a 6-layer convolutional neural network on MNIST [37], SVHN [38], CIFAR-10 [39], and TINYIMAGENET [40]. The training details can be found in Appendix A. We first present the main results and then justify our design choices with extensive ablation studies.

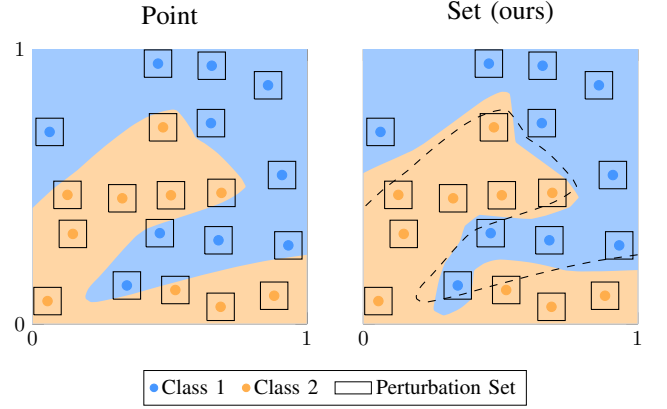


Fig. 7. Comparing the decision bounds of point-based (left) and set-based (right) training. The dashed line is the decision boundary of point-based training.

A. Main Results

We compare our set-based training against adversarial trade-off training, i.e., TRADES [23], as well as two state-of-the-art interval-based training approaches, i.e., IBP [7] and SABR [8]. For each training scheme, we report the clean accuracy, falsified accuracy (computed with PGD) [7], and, unlike previous works, the *fast-verified* accuracy. Most related works report verified accuracies computed with slow (exponential time) verification algorithms using branch-and-bound [8], [27], [28] or mixed-integer programming [7]; the verification can take up to 34h for MNIST networks [8, App. C]. Our goal is the fast (polynomial time) verification of neural networks. Thus, we report fast-verified accuracy using zonotopes.

Tab. I shows our results. Across all datasets, TRADES shows the best performance for clean and falsified accuracy; however, the verification is notoriously hard. Both interval-based approaches, IBP and SABR, have lower clean and falsified accuracy than TRADES but are significantly easier to verify. SABR achieves slightly better performance due to less regularization by propagating smaller intervals. For SVHN, SABR has lower verified accuracy than IBP, indicating that stronger verification algorithms are required. Our set-based training strikes a balance between TRADES and interval-based approaches, with significantly higher verified accuracy compared to TRADES and higher clean and falsified accuracy compared to IBP and SABR.

B. Understanding Robustness

To better understand the robustness of neural networks, we compare the learned decision boundaries of standard (point-based) and set-based training for a simple binary classification task (Fig. 7). Both training methods learn the training data perfectly, but set-based training pushes the decision boundaries away from the samples, making the set-based trained model more robust. For some samples, the decision boundary of the point-based trained neural network crosses their perturbation sets, which is not the case for the set-based trained neural network.

TABLE I
COMPARISON WITH STATE OF THE ART (MEAN & STD. DEV. OF THE BEST 3 RUNS ACROSS 5 SEEDS).

Dataset	ϵ_∞	Method	clean Acc.	falsified Acc.	fast-verified Acc. (max)	
MNIST	0.1	TRADES	99.40 \pm 0.04	98.40 \pm 0.06	0.00 \pm 0.00	(0.00)
		IBP	97.76 \pm 0.26	96.32 \pm 0.39	95.58 \pm 0.09	(96.05)
		SABR	97.94 \pm 0.44	95.84 \pm 1.28	92.80 \pm 1.88	(95.86)
		Set (ours)	98.76 \pm 0.29	97.54 \pm 0.22	95.86 \pm 0.82	(96.40)
CIFAR-10	$2/255$	TRADES	82.96 \pm 0.35	67.35 \pm 0.01	0.00 \pm 0.00	(0.00)
		IBP	46.54 \pm 2.92	42.13 \pm 2.56	36.83 \pm 1.74	(38.80)
		SABR	54.20 \pm 0.90	48.04 \pm 0.49	39.96 \pm 0.30	(40.30)
		Set (ours)	63.87 \pm 2.23	55.17 \pm 1.53	37.79 \pm 1.55	(39.36)
SVNH	0.01	TRADES	91.30 \pm 0.28	78.30 \pm 0.23	0.00 \pm 0.01	(0.01)
		IBP	72.33 \pm 4.26	61.27 \pm 3.46	46.93 \pm 3.09	(50.18)
		SABR	81.79 \pm 4.36	63.27 \pm 14.40	12.62 \pm 6.63	(17.81)
		Set (ours)	82.66 \pm 3.13	72.35 \pm 2.68	39.60 \pm 2.39	(41.35)
TINYIMAGENET	$1/255$	TRADES	28.14 \pm 0.56	19.80 \pm 0.43	0.00 \pm 0.00	(0.00)
		IBP	9.62 \pm 1.17	8.76 \pm 0.95	2.89 \pm 1.27	(4.07)
		SABR	13.74 \pm 1.38	12.49 \pm 1.25	3.68 \pm 0.87	(4.68)
		Set (ours)	16.70 \pm 2.79	14.80 \pm 2.54	0.02 \pm 0.02	(0.05)

TABLE II
PERFORMANCE ON MNIST FOR DIFFERENT WEIGHTING FACTORS IN THE SET-BASED LOSS (DEF. 5).

τ	clean Acc.	falsified Acc.	fast-verified Acc. (max)	
0.0	98.87 \pm 0.01	96.48 \pm 0.18	89.40 \pm 0.58	(90.04)
0.01	98.74 \pm 0.07	96.77 \pm 0.29	93.45 \pm 0.47	(93.73)
0.1	97.57 \pm 0.09	95.60 \pm 0.17	94.03 \pm 0.04	(94.06)
0.2	97.17 \pm 0.05	95.07 \pm 0.12	93.70 \pm 0.12	(93.82)
0.3	96.59 \pm 0.07	93.46 \pm 1.20	88.91 \pm 4.36	(93.95)

TABLE III
PERFORMANCE ON MNIST OF DIFFERENT INPUT SETS.

Method	clean Acc.	fast-verified Acc. (max)	
Set (ℓ_∞)	97.57 \pm 0.06	93.28 \pm 0.88	(93.89)
Set (FGSM)	98.15 \pm 0.06	95.46 \pm 0.55	(95.93)

C. Ablation Studies

We conduct ablation studies to justify our design choices. Please refer to Appendix A for details.

a) Weighting of Robustness Loss: The weighting factor τ in our set-based loss (Def. 5) can trade off accuracy with robustness. Tab. II shows the accuracies for different values of τ : For smaller values of τ , the clean accuracy is larger, and the verified accuracy is larger for larger values.

b) Input Set: Compared to other robust training approaches [7], [8], [27], our set-based training is not limited to multi-dimensional intervals as input sets. In Tab. III, we compare using the ℓ_∞ -ball as an input set with a smaller input set constructed with adversarial attacks (FGSM); see Appendix A for details. The smaller input set leads to better performance; thereby, we confirm the observations from previous works [8] that smaller input sets reduce the regularization by creating smaller approximation errors and thus having a better performance.

c) Set-Propagation Method: We justify the choice of using zonotopes and our image enclosure by comparing different set propagation methods for our set-based training (Tab. IV):

TABLE IV
PERFORMANCE ON MNIST OF DIFFERENT SET PROPAGATION METHODS.

Method	clean Acc.	falsified Acc.	fast-verified Acc.
Set (Our)	97.57 \pm 0.06	95.14 \pm 0.24	93.28 \pm 0.88
Set (Singh)	97.55 \pm 0.10	95.07 \pm 0.21	93.19 \pm 0.58
Set (IBP)	92.83 \pm 0.63	73.51 \pm 2.26	0.16 \pm 0.12

IBP, zonotopes with Singh’s enclosure, and zonotopes with our enclosure. We observe that our enclosure produces the best results. Due to large approximation errors, IBP achieves poor performance.

VI. CONCLUSION

This paper introduces the first set-based training procedure for neural networks that uses gradient sets: During training, we enclose the output set of the neural network using set propagation and derive a gradient set, which contains a different gradient for each possible output. By choosing gradients that point to the center of the output set, we can directly reduce the size of the output set. Thereby, we can simultaneously improve robustness and simplify the formal verification. The set-based training is made possible by a fast, batch-wise, and differentiable propagation of zonotopes which utilizes analytical solutions for approximation errors. Our experimental results demonstrate that our set-based approach effectively trains robust neural networks, which have competitive performance and admit fast verification (in polynomial time). Thereby, we demonstrate that gradient sets can be effectively used to train robust neural networks. Hence, set-based training represents a promising new direction for robust neural network training and a significant step toward fast verification of neural networks and, thus, the widespread adoption of formal verification of neural networks.

REFERENCES

- [1] G. Hinton, L. Deng, D. Yu, G. E. Dahl, A. Mohamed, N. Jaitly, A. Senior, V. Vanhoucke, P. Nguyen, T. N. Sainath, and B. Kingsbury,

- “Deep neural networks for acoustic modeling in speech recognition: The shared views of four research groups,” *IEEE Signal Process. Mag.*, vol. 29, no. 6, pp. 82–97, 2012.
- [2] C.-Y. Wang, A. Bochkovskiy, and H.-Y. M. Liao, “Yolov7: Trainable bag-of-freebies sets new state-of-the-art for real-time object detectors,” in *CVPR*, 2023, pp. 7464–7475.
- [3] C. Szegedy, W. Zaremba, I. Sutskever, J. Bruna, D. Erhan, I. Goodfellow, and R. Fergus, “Intriguing properties of neural networks,” in *ICLR*, 2014.
- [4] C. Ye, Y. Wang, Y. Wang, and M. Tie, “Steering angle prediction yolov5-based end-to-end adaptive neural network control for autonomous vehicles,” *Proc. Inst. Mech. Eng.*, vol. 236, no. 9, pp. 1991–2011, 2022.
- [5] A. Irfan, K. D. Julian, H. Wu, C. Barrett, M. J. Kochenderfer, B. Meng, and J. Lopez, “Towards verification of neural networks for small unmanned aircraft collision avoidance,” in *DASC*, 2020, pp. 1–10.
- [6] C. Brix, M. N. Müller, S. Bak, T. T. Johnson, and C. Liu, “First three years of the international verification of neural networks competition (VNN-COMP),” *STTT*, vol. 25, no. 3, pp. 329–339, 2023.
- [7] S. Gowal, K. Dvijotham, R. Stanforth, R. Bunel, C. Qin, J. Uesato, R. Arandjelovic, T. A. Mann, and P. Kohli, “Scalable verified training for provably robust image classification,” in *ICCV*, 2019, pp. 4841–4850.
- [8] M. N. Müller, F. Eckert, M. Fischer, and M. Vechev, “Certified training: Small boxes are all you need,” in *ICLR*, 2023.
- [9] G. Katz, C. Barrett, D. L. Dill, K. Julian, and M. J. Kochenderfer, “Reluplex: An efficient SMT solver for verifying deep neural networks,” in *CAV*, 2017, pp. 97–117.
- [10] G. Singh, T. Gehr, M. Püschel, and M. Vechev, “Boosting robustness certification of neural networks,” in *ICLR*, 2019.
- [11] H. Zhang, S. Wang, K. Xu, L. Li, B. Li, S. Jana, C.-J. Hsieh, and J. Z. Kolter, “General cutting planes for bound-propagation-based neural network verification,” *NeurIPS*, pp. 1656–1670, 2022.
- [12] R. Bunel, I. Turkaslan, P. H. S. Torr, M. P. Kumar, J. Lu, and P. Kohli, “Branch and bound for piecewise linear neural network verification,” *J. Mach. Learn. Res.*, vol. 21, no. 1, 2020.
- [13] C. Ferrari, M. N. Müller, N. Jovanović, and M. Vechev, “Complete verification via multi-neuron relaxation guided branch-and-bound,” in *ICLR*, 2022.
- [14] A. Girard, “Reachability of uncertain linear systems using zonotopes,” in *HSCC*, 2005, pp. 291–305.
- [15] T. Gehr, M. Mirman, D. Drachler-Cohen, P. Tsankov, S. Chaudhuri, and M. Vechev, “Ai2: Safety and robustness certification of neural networks with abstract interpretation,” in *IEEE SSP*, 2018, pp. 3–18.
- [16] G. Singh, T. Gehr, M. Mirman, M. Püschel, and M. Vechev, “Fast and effective robustness certification,” in *NeurIPS*, 2018.
- [17] N. Kochdumper, C. Schilling, M. Althoff, and S. Bak, “Open- and closed-loop neural network verification using polynomial zonotopes,” in *NFM*, 2023, pp. 16–36.
- [18] T. Ladner and M. Althoff, “Automatic abstraction refinement in neural network verification using sensitivity analysis,” in *HSCC*, 2023, pp. 1–13.
- [19] I. Goodfellow, J. Shlens, and C. Szegedy, “Explaining and harnessing adversarial examples,” in *ICLR*, 2015.
- [20] A. Kurakin, I. Goodfellow, and S. Bengio, “Adversarial machine learning at scale,” in *ICLR*, 2017.
- [21] A. Madry, A. Makelov, L. Schmidt, D. Tsipras, and A. Vladu, “Towards deep learning models resistant to adversarial attacks,” in *ICLR*, 2018.
- [22] L. Weng, H. Zhang, H. Chen, Z. Song, C.-J. Hsieh, L. Daniel, D. Boning, and I. Dhillon, “Towards fast computation of certified robustness for ReLU networks,” in *ICML*, 2018, pp. 5276–5285.
- [23] H. Zhang, Y. Yu, J. Jiao, E. Xing, L. E. Ghaoui, and M. Jordan, “Theoretically principled trade-off between robustness and accuracy,” in *ICML*, vol. 97, 2019, pp. 7472–7482.
- [24] H. Zhang, H. Chen, C. Xiao, S. Gowal, R. Stanforth, B. Li, D. S. Boning, and C. Hsieh, “Towards stable and efficient training of verifiably robust neural networks,” in *ICLR*, 2020.
- [25] E. Wong and Z. Kolter, “Provable defenses against adversarial examples via the convex outer adversarial polytope,” in *ICML*, 2018, pp. 5286–5295.
- [26] M. Mirman, T. Gehr, and M. Vechev, “Differentiable abstract interpretation for provably robust neural networks,” in *ICML*, 2018, pp. 3578–3586.
- [27] Y. Mao, M. Müller, M. Fischer, and M. Vechev, “Connecting certified and adversarial training,” in *NeurIPS*, 2023, pp. 73 422–73 440.
- [28] M. V. Mislav Balunović, “Adversarial training and provable defenses: Bridging the gap,” in *ICLR*, 2020.
- [29] Z. Shi, Y. Wang, H. Zhang, J. Yi, and C.-J. Hsieh, “Fast certified robust training with short warmup,” in *NeurIPS*, 2021, pp. 18 335–18 349.
- [30] C. M. Bishop, *Pattern recognition and machine learning*. Springer New York, NY, 2006.
- [31] X. Glorot and Y. Bengio, “Understanding the difficulty of training deep feedforward neural networks,” in *AISTATS*, 2010, pp. 249–256.
- [32] M. Althoff, “Reachability analysis and its application to the safety assessment of autonomous cars,” Ph.D. dissertation, Technische Universität München, 2010.
- [33] G. Elekes, “A geometric inequality and the complexity of computing volume,” *Discrete Comput. Geom.*, vol. 1, no. 4, pp. 289–292, 1986.
- [34] C. Combastel, “Zonotopes and Kalman observers: Gain optimality under distinct uncertainty paradigms and robust convergence,” *Automatica*, vol. 55, pp. 265–273, 2015.
- [35] H. Zhang, T.-W. Weng, P.-Y. Chen, C.-J. Hsieh, and L. Daniel, “Efficient neural network robustness certification with general activation functions,” in *NeurIPS*, 2018, pp. 4944–4953.
- [36] M. Althoff, “An introduction to CORA 2015,” in *ARCH Workshop*, 2015, pp. 120–151.
- [37] Y. LeCun, C. Cortes, and C. Burges, “MNIST handwritten digit database,” *ATT Labs [Online]*. Available: <http://yann.lecun.com/exdb/mnist>, vol. 2, 2010.
- [38] Y. Netzer, T. Wang, A. Coates, A. Bissacco, B. Wu, and A. Y. Ng, “Reading digits in natural images with unsupervised feature learning,” in *NIPS*, 2011.
- [39] A. Krizhevsky, “Learning multiple layers of features from tiny images,” Computer Science Department, University of Toronto, Tech. Rep., 2009.
- [40] Y. Le and X. Yang, “Tiny imagenet visual recognition challenge,” *CS 231N*, vol. 7, no. 7, p. 3, 2015.
- [41] D. P. Kingma and J. Ba, “Adam: A method for stochastic optimization,” in *ICLR*, 2015.
- [42] K. Xu, Z. Shi, H. Zhang, Y. Wang, K.-W. Chang, M. Huang, B. Kaillkura, X. Lin, and C.-J. Hsieh, “Automatic perturbation analysis for scalable certified robustness and beyond,” in *NeurIPS*, vol. 33, 2020, pp. 1129–1141.

APPENDIX A EVALUATION DETAILS

a) *Hardware*: Our experiments were run on a server with $2 \times$ AMD EPYC 7763 (64 cores/128 threads), 2TB RAM, and a NVIDIA A100 40GB GPU.

b) *Training Hyperparameters*: The training hyperparameters are listed in Tab. V and the neural network architectures in Tab. VI. We use the same notation as [7]: $\text{CONV } k \ w \times h + s$ denotes a convolutional layer with k filters of size $w \times h$ and stride s , and $\text{FC } n$ denotes a fully connected layer with n neurons. The weights and biases are initialized as in [29]. We use Adam optimizer [41] with the recommended hyperparameters. For all training methods, we tried to use hyperparameters as close as possible to the reported hyperparameters in their respective paper: for [7] we use $\kappa = 1/2$, for [23] we use $1/\lambda = 6$, for [8] we use $\lambda = 0.1$ for CIFAR-10, and $\lambda = 0.4$ for MNIST and SVHN. For [7], [8] we omit the ReLU warm-up regularization. For any PGD during training (used by methods [8], [21], [23]) we used the settings from [8]: 8 iterations with an initial step size 0.5, which is decayed twice by 0.1 at iterations 4 and 7. All PGD attacks for testing are computed with 40 iterations of step size 0.01. Moreover, all reported accuracies are averaged over the best 3 of 5 runs. We clip gradients with a ℓ_2 -norm of greater than 10. All reported perturbation radii are w.r.t. normalized inputs between 0 and 1. To reduce computational resources, we perform the ablation studies with a smaller 3-layer convolutional neural network trained on MNIST.

c) *Datasets*: MNIST contains 60 000 grayscale images of size 28×28 . Each image depicts a handwritten digit from 0 to 9. SVHN is a real-world dataset that contains 73 257 colored

TABLE V
TRAINING HYPERPARAMETERS.

Dataset	η	ϵ	τ	Batch Size	#Epochs (warm-up / ramp-up)	Decay
MNIST	$5 \cdot 10^{-4}$	0.1	0.1	256	70 (1/20)	50, 60
CIFAR-10	$5 \cdot 10^{-4}$	$2/255$	0.005	128	160 (40/120)	120, 140
SVHN	$5 \cdot 10^{-4}$	0.01	0.01	128	70 (20/50)	50, 60
TINYIMAGENET	$5 \cdot 10^{-4}$	$1/255$	0.1	64	70 (20/50)	50, 60

TABLE VI
NEURAL NETWORK ARCHITECTURES. EACH LINEAR LAYER OR CONVOLUTIONAL LAYER (EXCEPT THE LAST LAYER) IS FOLLOWED BY A BATCH NORMALIZATION AND A NONLINEAR ACTIVATION LAYER (ReLU).

CNN3	CNN6
CONV $5 \ 4 \times 4 + 2$	CONV $32 \ 3 \times 3 + 1$
CONV $10 \ 4 \times 4 + 1$	CONV $32 \ 4 \times 4 + 2$
FC 100	CONV $64 \ 3 \times 3 + 1$
	CONV $64 \ 4 \times 4 + 2$
	FC 512
	FC 512

images of digits of house numbers that are cropped to size 32×32 . The CIFAR-10 dataset contains 60 000 colored images of size 32×32 . The TINYIMAGENET data set contains 100 000 colored images of size 64×64 labeled with 200 classes. We use the canonical split of training and test data for each dataset and the entire test data for evaluation; because test labels are not available for TINYIMAGENET, we follow [8] and use the validation set for testing. Following [42], we augment the CIFAR-10 and TINYIMAGENET dataset with random crop and flips. The perturbation is applied before the normalization to ensure comparability with the literature.

d) Improvements for Scalability: The complexity of our set-based training depends on the number of generators of the output set used during training (Prop. 14). We use two methods to reduce the number of generators: (i) We propagate the approximation errors as intervals through the neural network and compute the Minkowski sum at the end. (ii) We use input sets with fewer number of generators. Our set-based training can use any zonotopic input set and is not limited to ℓ_∞ -input sets. Building on previous work [8], we use adversarial attacks to construct smaller input sets that focus on critical regions of the input; thereby, the regularization through large approximation errors is reduced. Previous works only use a single adversarial attack to construct a smaller ℓ_∞ -input set [8]. We extend this idea and use several adversarial attacks to construct zonotopic input sets: We shift the center of the input set to the average attack and use scaled directions of the attacks as generators for the input set. Given an input $x \in \mathbb{R}^{n_0}$, we compute λ adversarial attacks $\tilde{x}_i = x + \delta_i$ for $i \in [\lambda]$ (e.g., using FGSM). The input set is constructed as

$$\mathcal{X} = \left\langle x + 1/\lambda \sum_{i=1}^{\lambda} \delta_i, 1/\lambda [\delta_1 \quad \delta_2 \quad \cdots \quad \delta_\lambda] \right\rangle_Z$$

e) Fairness: We note that compared to the literature, we use smaller neural networks and compare the means across several training runs; most literature only reports

TABLE VII
TRAINING TIME WITH CNN6 ON MNIST (MIN. OF 5 RUNS) [SEC / EPOCH].

Method	Training Time [sec / Epoch]
Point	6.1
TRADES	49.6
IBP	19.9
SABR	52.0
Set (ours)	61.2

their best-observed scores, which is problematic regarding reproducibility and fairness, because it is unclear how many training seed were used. Therefore, to create a fair comparison, we reimplement related approaches [7], [8], [21], [23]. The implementations are validated by reproducing their reported results.

f) Training Times: A comparison of the training times is shown in Tab. VII.

APPENDIX B PROOFS

Proposition 9. *The approximation error of p for $\phi \in \{\text{ReLU}, \tanh, \sigma\}$ are computed as*

$$\underline{d} = \min_{x \in \mathcal{P}_\phi \cap [l, u]} \phi(x) - p(x), \quad \bar{d} = \max_{x \in \mathcal{P}_\phi \cap [l, u]} \phi(x) - p(x),$$

where

$$\begin{aligned} \mathcal{P}_{\text{ReLU}} &= \{0, l, u\}, \\ \mathcal{P}_{\tanh} &= \{\pm \tanh^{-1}(\sqrt{1-a}), l, u\}, \text{ and} \\ \mathcal{P}_\sigma &= \{\pm 2 \tanh^{-1}(\sqrt{1-4a}), l, u\}. \end{aligned}$$

Proof. Case (i). $\phi = \text{ReLU}$. $\text{ReLU}(x) - p(x)$ is linear for $[l, 0]$ and $[0, u]$. Thus, the approximation errors are found at the bounds $x \in \{l, u\}$ or where $0 \in [l, u]$ at $x = 0$.

Case (ii). $\phi = \tanh$. The derivative of the hyperbolic tangent is $\tanh'(x) = 1 - \tanh(x)^2$. To compute the extreme points of $\tanh(x) - p(x)$, we demand that its derivative is 0 and simplify the terms:

$$\begin{aligned} 0 &\stackrel{!}{=} d/dx(\tanh(x) - p(x)) \\ \Leftrightarrow 0 &= 1 - \tanh(x)^2 - a \\ \Leftrightarrow x &= \pm \tanh^{-1}(\sqrt{1-a}). \quad \square \end{aligned}$$

Case (iii). $\phi = \sigma$. To compute the extreme points of $\sigma(x) - p(x)$, we demand that its derivative is 0 and simplify the terms:

$$\begin{aligned} 0 &\stackrel{!}{=} d/dx(\sigma(x) - p(x)) \\ \Leftrightarrow 0 &= d/dx(1/2(\tanh(x/2) + 1) - p(x)) \\ \Leftrightarrow x &= \pm 2 \tanh^{-1}(\sqrt{1-4a}). \end{aligned}$$

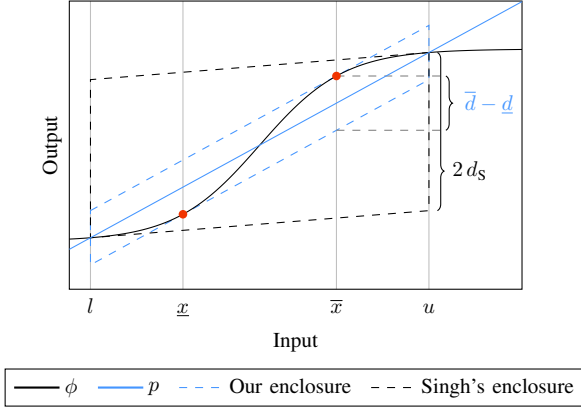


Fig. 8. Illustration for Theorem 1.

Theorem 1. Let ϕ be an s -shaped function, and let $[l, u]$ be an interval. Moreover, let \underline{d} and \bar{d} be the approximation errors of p as defined in Prop. 9 and Def. 7, and let d_S be the approximation error of Singh's enclosure [16, Thm. 3.2]. It holds that

$$\text{area}([\underline{d}, \bar{d}], [l, u]) \leq \text{area}([-d_S, d_S], [l, u]).$$

Proof. We first observe that the approximation errors \underline{d} and \bar{d} of p can be computed at points $\underline{x}, \bar{x} \in [l, u]$ such that $\underline{x} \leq \bar{x}$ (Fig. 8):

$$\underline{d} = \phi(\underline{x}) - p(\underline{x}), \quad \bar{d} = \phi(\bar{x}) - p(\bar{x}). \quad (12)$$

Singh's enclosure [16, Thm. 3.2] uses the linear approximation $p_S(x) = a_S x + b_S$, with slope a_S , offset b_S , and approximation error d_S :

$$\begin{aligned} a_S &= \min(\phi'(l), \phi'(u)) \\ b_S &= 1/2 (\phi(u) + \phi(l) - a_S(u + l)) \\ d_S &= 1/2 (\phi(u) - \phi(l) - a_S(u - l)). \end{aligned} \quad (13)$$

With Def. 7, we have the following inequality:

$$a = \frac{\phi(u) - \phi(l)}{u - l} \geq a_S.$$

Hence, we have

$$a(\bar{x} - \underline{x}) \geq a_S(\bar{x} - \underline{x}). \quad (14)$$

Moreover, from (13) we have for all $x \in [l, u]$:

$$\begin{aligned} \phi(x) - \phi(l) &\geq a_S(x - l) \\ \implies \phi(\underline{x}) &\geq \phi(l) + a_S(\underline{x} - l), \\ \phi(u) - \phi(x) &\geq a_S(u - x) \\ \implies \phi(\bar{x}) &\leq \phi(u) - a_S(u - \bar{x}). \end{aligned} \quad (15)$$

Ultimately, we have

$$\begin{aligned} \bar{d} - \underline{d} &\stackrel{(12)}{=} \phi(\bar{x}) - p(\bar{x}) - (\phi(\underline{x}) - p(\underline{x})) \\ &\stackrel{\text{Def. 7}}{=} \phi(\bar{x}) - (a\bar{x}) - (\phi(\underline{x}) - (a\underline{x})) \\ &\stackrel{(14)}{\leq} \phi(\bar{x}) - \phi(\underline{x}) - a_S(\bar{x} - \underline{x}) \\ &\stackrel{(15)}{\leq} \phi(u) - a_S(u - \bar{x}) - (\phi(l) + a_S(\underline{x} - l)) \\ &\quad - a_S(\bar{x} - \underline{x}) \\ &\stackrel{(13)}{=} 2d_S. \end{aligned} \quad (16)$$

Hence, we obtain the bound $\bar{d} - \underline{d} \leq 2d_S$. Thus,

$$\begin{aligned} \text{area}([\underline{d}, \bar{d}], [l, u]) &\stackrel{(8)}{=} (u - l)(\bar{d} - \underline{d}) \stackrel{(16)}{\leq} (u - l)2d_S \\ &\stackrel{(8)}{=} \text{area}([-d_S, d_S], [l, u]). \end{aligned} \quad (17)$$

□

Proposition 13. For an input set $\mathcal{H}_{k-1} = \langle c, G \rangle_Z$ with $c \in \mathbb{R}^n$ and $G \in \mathbb{R}^{n \times q}$, Alg. 1 has time complexity $\mathcal{O}(n^2 q)$ w.r.t. the number of input dimensions n and the number of generators q .

Proof. Finding the interval bounds of \mathcal{H}_{k-1} (line 2) takes time $\mathcal{O}(nq)$ (Prop. 2). Computing the linear approximation (line 4) and the approximation errors (line 5) for each neuron takes constant time; hence, the loop takes time $\mathcal{O}(n)$. The linear map of \mathcal{H}_{k-1} (line 6) takes time $\mathcal{O}(n^2 q)$ (Prop. 4). Adding the approximation errors (line 7) takes time $\mathcal{O}(n)$. Thus, in total we have $\mathcal{O}(nq) + \mathcal{O}(n) + \mathcal{O}(n^2 q) + \mathcal{O}(n) = \mathcal{O}(n^2 q)$. □

Proposition 7. The gradient of the F-radius is

$$\nabla_{\mathcal{Y}} \|\mathcal{Y}\|_F = \frac{1}{n_{\kappa} \|\mathcal{Y}\|_F} \langle \mathbf{0}, G_{\kappa} \rangle_Z,$$

where $\mathcal{Y} = \langle c_{\kappa}, G_{\kappa} \rangle_Z \subset \mathbb{R}^{n_{\kappa}}$.

Proof. The center does not affect the F-radius, hence $\nabla_{c_{\kappa}} \|\mathcal{Y}\|_F = \mathbf{0}$. The F-radius is the sum of all squared entries of the generator matrix. Hence,

$$\nabla_{G_{\kappa}} \|\mathcal{Y}\|_F = \frac{1}{n_{\kappa}} \nabla_{G_{\kappa}} \sqrt{\mathbf{1}^{\top} (G_{\kappa} \odot G_{\kappa}) \mathbf{1}} = \frac{G_{\kappa}}{n_{\kappa} \|\mathcal{Y}\|_F}. \quad (18)$$

Thus,

$$\begin{aligned} \nabla_{\mathcal{Y}} \|\mathcal{Y}\|_F &\stackrel{\text{Def. 3}}{=} \langle \nabla_{c_{\kappa}} \|\mathcal{Y}\|_F, \nabla_{G_{\kappa}} \|\mathcal{Y}\|_F \rangle_Z \\ &\stackrel{(18)}{=} \left\langle \mathbf{0}, \frac{G_{\kappa}}{n_{\kappa} \|\mathcal{Y}\|_F} \right\rangle_Z = \frac{1}{n_{\kappa} \|\mathcal{Y}\|_F} \langle \mathbf{0}, G_{\kappa} \rangle_Z. \quad \square \end{aligned}$$

We first prove the correctness of the gradient of the set-based loss.

Proposition 8 (Set-Based Loss Gradient). The gradient of the set-based loss function \mathcal{L} is

$$\nabla_{\mathcal{Y}} \mathcal{L}(t, \mathcal{Y}) = \left\langle (1 - \tau) \nabla_{c_{\kappa}} L(t, c_{\kappa}), \frac{\tau}{\epsilon n_{\kappa} \|\mathcal{Y}\|_F} G_{\kappa} \right\rangle_Z,$$

where $\mathcal{Y} = \langle c_{\kappa}, G_{\kappa} \rangle_Z \subset \mathbb{R}^{n_{\kappa}}$.

Proof. This follows from Def. 5 and Prop. 7:

$$\begin{aligned} \nabla_{\mathcal{Y}} \mathcal{L}(t, \mathcal{Y}) &\stackrel{\text{Def. 5}}{=} (1 - \tau) \nabla_{\mathcal{Y}} L(t, c_{\kappa}) + \frac{\tau}{\epsilon} \nabla_{\mathcal{Y}} \|\mathcal{Y}\|_F \\ &\stackrel{\text{Def. 3}}{=} (1 - \tau) \langle \nabla_{c_{\kappa}} L(t, c_{\kappa}), \mathbf{0} \rangle_Z \\ &\quad + \frac{\tau}{\epsilon} \nabla_{\mathcal{Y}} \|\mathcal{Y}\|_F \\ &\stackrel{\text{Prop. 7}}{=} (1 - \tau) \langle \nabla_{c_{\kappa}} L(t, c_{\kappa}), \mathbf{0} \rangle_Z \\ &\quad + \frac{\tau}{\epsilon n_{\kappa} \|\mathcal{Y}\|_F} \langle \mathbf{0}, G_{\kappa} \rangle_Z \\ &= \left\langle (1 - \tau) \nabla_{c_{\kappa}} L(t, c_{\kappa}), \frac{\tau}{\epsilon n_{\kappa} \|\mathcal{Y}\|_F} G_{\kappa} \right\rangle_Z. \quad \square \end{aligned}$$

Moreover, in this section, we give three proofs for the set-based backpropagation: (i) set-based backpropagation through

an image enclosure (Prop. 10), (ii) set-based backpropagation through all layers of a neural network (Prop. 11), and (iii) set-based weight and bias update (Prop. 12).

Before we prove the propositions required for the set-based backpropagation, we unfold (9) and rewrite the gradient set \mathcal{G}_{k-1} using the chain rule for partial derivatives. Let $\mathcal{H}_k = \langle c_k, G_k \rangle_Z$ with $G_k \in \mathbb{R}^{n_k \times q}$ be the output set of the k -th layer and let $\mathcal{G}_k = \langle c'_k, G'_k \rangle_Z$ be the gradient set w.r.t. \mathcal{H}_k :

$$\begin{aligned} \mathcal{G}_{k-1} &\stackrel{(9)}{=} \nabla_{\mathcal{H}_{k-1}} \mathcal{L}(t, \mathcal{Y}) \\ &= \sum_{i=1}^{n_k} \frac{\partial \mathcal{L}(t, \mathcal{Y})}{\partial c_{k(i)}} \nabla_{\mathcal{H}_{k-1}} c_{k(i)} \\ &\quad + \sum_{i=1}^{n_k} \sum_{j=1}^q \frac{\partial \mathcal{L}(t, \mathcal{Y})}{\partial G_{k(i,j)}} \nabla_{\mathcal{H}_{k-1}} G_{k(i,j)} \\ &= \sum_{i=1}^{n_k} c'_{k(i)} \nabla_{\mathcal{H}_{k-1}} c_{k(i)} \\ &\quad + \sum_{i=1}^{n_k} \sum_{j=1}^q G'_{k(i,j)} \nabla_{\mathcal{H}_{k-1}} G_{k(i,j)}. \end{aligned} \quad (19)$$

Note: the plus symbol (+) between zonotopes denotes their element-wise addition: $\langle c_1, G_1 \rangle_Z + \langle c_2, G_2 \rangle_Z = \langle c_1 + c_2, G_1 + G_2 \rangle_Z$, whereas the Minkowski sum is denoted as $\langle c_1, G_1 \rangle_Z \oplus \langle c_2, G_2 \rangle_Z = \langle c_1 + c_2, [G_1 \ G_2] \rangle_Z$.

Proposition 10 (Backpropagation through Image Enclosure). *Assume the k -th layer is a nonlinear layer with activation function ϕ_k . Given an input set $\mathcal{H}_{k-1} = \langle c_{k-1}, G_{k-1} \rangle_Z$ with $G_{k-1} \in \mathbb{R}^{n_{k-1} \times p}$ and a gradient set $\mathcal{G}_k = \langle c'_k, G'_k \rangle_Z$, the gradient set $\mathcal{G}_{k-1} = \langle c'_{k-1}, G'_{k-1} \rangle_Z$ is computed for each dimension $i \in [n_k]$ as*

$$\begin{aligned} \mathcal{G}_{k-1(i)} &= \left(c'_{k(i)} c_{k-1(i)} + G'_{k(i,[p])} G_{k-1(i,\cdot)}^\top \right) \nabla_{\mathcal{H}_{k-1(i)}} a_{k(i)} \\ &\quad + \mathcal{G}_{k(i)} a_{k(i)} + c'_{k(i)} \nabla_{\mathcal{H}_{k-1(i)}} d_{c,k(i)} \\ &\quad + G'_{k(i,p+i)} \nabla_{\mathcal{H}_{k-1(i)}} d_k(i). \end{aligned}$$

The operation `backpropEnclose` computes the gradient set of our image enclosure (Prop. 10).

Proof. The image enclosure adds n_k generators, hence the input set \mathcal{H}_{k-1} has n_k generators less than gradient set \mathcal{G}_k , i.e. $G_{k-1} \in \mathbb{R}^{n_k \times p}$ and $G'_k \in \mathbb{R}^{n_k \times q}$ with $q = p + n_k$. We split (19) into three summands:

$$\begin{aligned} \mathcal{G}_{k-1,c} &= \sum_{i=1}^{n_k} c'_{k(i)} \nabla_{\mathcal{H}_{k-1}} c_{k(i)}, \\ \mathcal{G}_{k-1,p} &= \sum_{i=1}^{n_k} \sum_{j=1}^p G'_{k(i,j)} \nabla_{\mathcal{H}_{k-1}} G_{k(i,j)}, \\ \mathcal{G}_{k-1,q} &= \sum_{i=1}^{n_k} \sum_{j=p+1}^q G'_{k(i,j)} \nabla_{\mathcal{H}_{k-1}} G_{k(i,j)}. \end{aligned}$$

Hence,

$$\mathcal{G}_{k-1} = \mathcal{G}_{k-1,c} + \mathcal{G}_{k-1,p} + \mathcal{G}_{k-1,q}. \quad (20)$$

Furthermore, the input set \mathcal{H}_{k-1} is enclosed by the interval $[l_{k-1}, u_{k-1}]$, where $l_{k-1} = c_{k-1} - |G_{k-1}| \mathbf{1}$ and $u_{k-1} =$

$c_{k-1} + |G_{k-1}| \mathbf{1}$ (Prop. 2). Moreover, let $e_i \in \{0, 1\}^{n_k}$ be the i -th standard basis vector.

Firstly, we derive the gradient $\nabla_{\mathcal{H}_{k-1}} c_{k(i)}$ needed for $\mathcal{G}_{k-1,c}$, for which we need the gradients of center $c_{k(i)} = a_{k(i)} c_{k-1(i)} + d_{c,k(i)}$ w.r.t. the input set \mathcal{H}_{k-1} for each dimension $i \in [n_k]$. The image enclosure is applied for each dimension individually; therefore, we can consider each dimension separately because for any dimensions $i, j \in [n_{k-1}]$, where $i \neq j$:

$$\nabla_{\mathcal{H}_{k-1(j)}} c_{k(i)} = \langle 0, \mathbf{0} \rangle_Z, \quad \nabla_{\mathcal{H}_{k-1(j)}} G_{k(i,\cdot)} = \langle 0, \mathbf{0} \rangle_Z. \quad (21)$$

Let $i \in [n_k]$ be a fixed dimension and $j \in [p]$ a fixed index of a generator. We require the gradient of the slope $a_{k(i)}$ and the offset $d_{c,k(i)}$. The gradient of the slope $a_{k(i)}$ is:

$$\begin{aligned} \frac{\partial a_{k(i)}}{\partial c_{k-1(i)}} &\stackrel{\text{Def. 7}}{=} \frac{\phi'(u_{k-1(i)}) - \phi'(l_{k-1(i)})}{u_{k-1(i)} - l_{k-1(i)}}, \\ \frac{\partial a_{k(i)}}{\partial G_{k-1(i,j)}} &\stackrel{\text{Def. 7}}{=} \left(\frac{\phi'(u_{k-1(i)}) + \phi'(l_{k-1(i)}) - 2 a_{k(i)}}{u_{k-1(i)} - l_{k-1(i)}} \right) \\ &\quad \cdot \text{sign}(G_{k-1(i,j)}). \end{aligned}$$

Let \bar{x}_k and \underline{x}_k be the points of the approximation errors \bar{d}_k and \underline{d}_k :

$$\begin{aligned} \bar{x}_k &= \arg \max_{x \in \mathcal{P}} \phi_k(x) - p_k(x), \\ \underline{x}_k &= \arg \min_{x \in \mathcal{P}} \phi_k(x) - p_k(x). \end{aligned}$$

To prevent repetitions in this proof, let g denote the center, or an arbitrary generator of the input set \mathcal{H}_{k-1} :

$$g \in \{c_{k-1}, G_{k-1(\cdot,1)}, G_{k-1(\cdot,2)}, \dots, G_{k-1(\cdot,p)}\}.$$

For $(x, d) \in \{(\bar{x}_k, \bar{d}_k), (\underline{x}_k, \underline{d}_k)\}$, we apply the chain rule and the product-rule to derive the gradients of the approximation error $d_{(i)}$:

$$\begin{aligned} \frac{\partial d_{(i)}}{\partial g_{(i)}} &= \frac{\partial (\phi_k(x_{(i)}) - a_{k(i)} x_{(i)})}{\partial g_{(i)}} \\ &= (\phi'_k(x_{(i)}) - a_{k(i)}) \frac{\partial x_{(i)}}{\partial g_{(i)}} - \frac{\partial a_{k(i)}}{\partial g_{(i)}} x_{(i)}. \end{aligned}$$

Please recall the offset $d_{c,k} = 1/2 (\bar{d}_k + \underline{d}_k)$ and approximation error $d_k = 1/2 (\bar{d}_k - \underline{d}_k)$ (Prop. 9); hence,

$$\begin{aligned} \frac{\partial d_{c,k(i)}}{\partial g_{(i)}} &= \frac{1}{2} \left(\frac{\partial \bar{d}_{k(i)}}{\partial g_{(i)}} + \frac{\partial \underline{d}_{k(i)}}{\partial g_{(i)}} \right), \\ \frac{\partial d_{k(i)}}{\partial g_{(i)}} &= \frac{1}{2} \left(\frac{\partial \bar{d}_{k(i)}}{\partial g_{(i)}} - \frac{\partial \underline{d}_{k(i)}}{\partial g_{(i)}} \right). \end{aligned}$$

Using the gradient of the slope $a_{k(i)}$ and the gradient of the offset $d_{c,k(i)}$, we derive the gradient of the center $c_{k(i)}$:

$$\begin{aligned}\frac{\partial c_{k(i)}}{\partial c_{k-1(i)}} &= \frac{\partial(a_{k(i)} c_{k-1(i)} + d_{c,k(i)})}{\partial c_{k-1(i)}} \\ &= a_{k(i)} + \frac{\partial a_{k(i)}}{\partial c_{k-1(i)}} c_{k-1(i)} + \frac{\partial d_{c,k(i)}}{\partial c_{k-1(i)}}, \\ \frac{\partial c_{k(i)}}{\partial G_{k-1(i,j)}} &= \frac{\partial(a_{k(i)} c_{k-1(i)} + d_{c,k(i)})}{\partial G_{k-1(i,j)}} \\ &= \frac{\partial a_{k(i)}}{\partial G_{k-1(i,j)}} c_{k-1(i)} + \frac{\partial d_{c,k(i)}}{\partial G_{k-1(i,j)}}.\end{aligned}$$

Hence, we have

$$\begin{aligned}\nabla_{\mathcal{H}_{k-1(i)}} c_{k(i)} &= \left\langle \frac{\partial c_{k(i)}}{\partial c_{k-1(i)}}, \frac{\partial c_{k(i)}}{\partial G_{k-1(i,\cdot)}} \right\rangle_Z \\ &= a_{k(i)} + \nabla_{\mathcal{H}_{k-1(i)}} a_{k(i)} c_{k-1(i)} \\ &\quad + \nabla_{\mathcal{H}_{k-1(i)}} d_{c,k(i)}.\end{aligned}\quad (22)$$

Secondly, we derive the gradient $\nabla_{\mathcal{H}_{k-1(i)}} G_{k(i,j)}$ needed for $\mathcal{G}_{k-1,p}$. Let $j' \in [n_k]$ be a different generator index: $j' \neq j$; the gradient of $G_{k(i,j)}$ is

$$\begin{aligned}\frac{\partial G_{k(i,j)}}{\partial c_{k-1(i)}} &= \frac{\partial(a_{k(i)} G_{k-1(i,j)})}{\partial c_{k-1(i)}} = \frac{\partial a_{k(i)}}{\partial c_{k-1(i)}} G_{k-1(i,j)}, \\ \frac{\partial G_{k(i,j)}}{\partial G_{k-1(i,j)}} &= \frac{\partial(a_{k(i)} G_{k-1(i,j)})}{\partial G_{k-1(i,j)}} \\ &= a_{k(i)} + \frac{\partial a_{k(i)}}{\partial G_{k-1(i,j)}} G_{k-1(i,j)}, \\ \frac{\partial G_{k(i,j)}}{\partial G_{k-1(i,j')}} &= \frac{\partial(a_{k(i)} G_{k-1(i,j)})}{\partial G_{k-1(i,j')}} = \frac{\partial a_{k(i)}}{\partial G_{k-1(i,j')}} G_{k-1(i,j)}.\end{aligned}$$

Hence, we have

$$\begin{aligned}\nabla_{\mathcal{H}_{k-1(i)}} G_{k(i,j)} &= \left\langle \frac{\partial G_{k(i,j)}}{\partial c_{k-1(i)}}, \frac{\partial G_{k(i,j)}}{\partial G_{k-1(i,\cdot)}} \right\rangle_Z \\ &= \nabla_{\mathcal{H}_{k-1(i)}} a_{k(i)} G_{k-1(i,j)} \\ &\quad + a_{k(i)} \langle \mathbf{0}, e_i e_j^\top \rangle_Z.\end{aligned}\quad (23)$$

Thirdly, we derive $\mathcal{G}_{k-1,q}$. Please recall, the diagonal entries of $G_{k(\cdot, p+[n_k])}$ contain the approximation errors, while the non-diagonal entries are 0; hence, the gradient of any non-diagonal entry $j' \in [q]: j' > p \wedge j' \neq p+i$ is 0: $\nabla_{\mathcal{H}_{k-1(i)}} G_{k(i,j')} = \langle \mathbf{0}, \mathbf{0} \rangle_Z$. Hence, we can simplify $\mathcal{G}_{k-1,q}$:

$$\begin{aligned}\mathcal{G}_{k-1,q(i)} &= \sum_{j=p+1}^q G'_{k(i,j)} \nabla_{\mathcal{H}_{k-1(i)}} G_{k(i,j)} \\ &= G'_{k(i,p+i)} \nabla_{\mathcal{H}_{k-1(i)}} d_{k(i)}.\end{aligned}\quad (24)$$

We add $\mathcal{G}_{k-1,c}$ and $\mathcal{G}_{k-1,p}$ together and reorder the terms:

$$\begin{aligned}\mathcal{G}_{k-1,c(i)} + \mathcal{G}_{k-1,p(i)} &= c'_{k(i)} \nabla_{\mathcal{H}_{k-1(i)}} c_{k(i)} + \sum_{j=1}^p G'_{k(i,j)} \nabla_{\mathcal{H}_{k-1(i)}} G_{k(i,j)} \\ &\stackrel{(22)}{=} c'_{k(i)} (a_{k(i)} + \nabla_{\mathcal{H}_{k-1(i)}} a_{k(i)} c_{k-1(i)} + \nabla_{\mathcal{H}_{k-1(i)}} d_{c,k(i)}) \\ &\quad + \sum_{j=1}^p G'_{k(i,j)} \nabla_{\mathcal{H}_{k-1(i)}} G_{k(i,j)} \\ &\stackrel{(23)}{=} c'_{k(i)} (a_{k(i)} + \nabla_{\mathcal{H}_{k-1(i)}} a_{k(i)} c_{k-1(i)} + \nabla_{\mathcal{H}_{k-1(i)}} d_{c,k(i)}) \\ &\quad + \sum_{j=1}^p G'_{k(i,j)} (\nabla_{\mathcal{H}_{k-1(i)}} a_{k(i)} G_{k-1(i,j)} + a_{k(i)} \langle \mathbf{0}, e_i e_j^\top \rangle_Z) \\ &= \nabla_{\mathcal{H}_{k-1(i)}} a_{k(i)} (c_{k-1(i)} c'_{k(i)} + G_{k-1(i,\cdot)}^\top G'_{k(i,[p])}) \\ &\quad + \mathcal{G}_{k(i)} a_{k(i)} + c'_{k(i)} \nabla_{\mathcal{H}_{k-1(i)}} d_{c,k(i)}.\end{aligned}\quad (25)$$

Finally, we obtain

$$\begin{aligned}\mathcal{G}_{k-1(i)} &\stackrel{(20)}{=} \mathcal{G}_{k-1,c(i)} + \mathcal{G}_{k-1,p(i)} + \mathcal{G}_{k-1,q(i)} \\ &\stackrel{(25)}{=} \nabla_{\mathcal{H}_{k-1(i)}} a_{k(i)} (c_{k-1(i)} c'_{k(i)} + G_{k-1(i,[p])}^\top G'_{k(i,[p])}) \\ &\quad + \mathcal{G}_{k(i)} a_{k(i)} + c'_{k(i)} \nabla_{\mathcal{H}_{k-1(i)}} d_{c,k(i)} + \mathcal{G}_{k-1,q(i)} \\ &\stackrel{(24)}{=} \nabla_{\mathcal{H}_{k-1(i)}} a_{k(i)} (c_{k-1(i)} c'_{k(i)} + G_{k-1(i,[p])}^\top G'_{k(i,[p])}) \\ &\quad + \mathcal{G}_{k(i)} a_{k(i)} + c'_{k(i)} \nabla_{\mathcal{H}_{k-1(i)}} d_{c,k(i)} \\ &\quad + G'_{k(i,p+i)} \nabla_{\mathcal{H}_{k-1(i)}} d_{k(i)}.\end{aligned}\quad \square$$

Proposition 11 (Set-Based Backpropagation). *The gradient sets \mathcal{G}_k are computed in reverse order as*

$$\begin{aligned}\mathcal{G}_\kappa &= \nabla_{\mathcal{Y}} \mathcal{L}(t, \mathcal{Y}), \\ \mathcal{G}_{k-1} &= \begin{cases} W_k^\top \mathcal{G}_k & \text{if } k\text{-th layer is linear,} \\ \text{backpropEnclose}(\phi_k, \mathcal{G}_k) & \text{otherwise,} \end{cases}\end{aligned}$$

for all $k \in \{\kappa, \dots, 1\}$.

Proof. If $k = \kappa$, we compute the gradient of the set-based loss according to Prop. 8. We assume $k < \kappa$. Let $\mathcal{G}_k = \langle c'_k, G'_k \rangle_Z$ and $\mathcal{H}_k = \langle c_k, G_k \rangle_Z$.

We split cases on the type of the k -th layer and simplify the terms.

Case (i). The k -th layer is linear. For dimension $i \in [n_k]$, we have

$$\begin{aligned}\nabla_{\mathcal{H}_{k-1}} c_{k(i)} &= \nabla_{\mathcal{H}_{k-1}} (W_{k(i,\cdot)} c_{k-1} + b_{k(i)}) \\ &= \left\langle W_{k(i,\cdot)}^\top, \mathbf{0} \right\rangle_Z, \\ \nabla_{\mathcal{H}_{k-1}} G_{k(i,j)} &= \nabla_{\mathcal{H}_{k-1}} (W_{k(i,\cdot)} G_{k-1(\cdot,j)}) \\ &= \left\langle \mathbf{0}, W_{k(i,\cdot)}^\top e_j^\top \right\rangle_Z.\end{aligned}\quad (26)$$

Thus,

$$\begin{aligned}
\mathcal{G}_{k-1} &\stackrel{(19)}{=} \sum_{i=1}^{n_k} c'_{k(i)} \nabla_{\mathcal{H}_{k-1}} c_{k(i)} \\
&\quad + \sum_{i=1}^{n_k} \sum_{j=1}^q G'_{k(i,j)} \nabla_{\mathcal{H}_{k-1}} G_{k(i,j)} \\
&\stackrel{(26)}{=} \sum_{i=1}^{n_k} c'_{k(i)} \left\langle W_{k(i,\cdot)}^\top, \mathbf{0} \right\rangle_Z \\
&\quad + \sum_{i=1}^{n_k} \sum_{j=1}^q G'_{k(i,j)} \left\langle \mathbf{0}, W_{k(i,\cdot)}^\top e_j^\top \right\rangle_Z \\
&= \left\langle \sum_{i=1}^{n_k} W_{k(i,\cdot)}^\top c'_{k(i)}, \sum_{i=1}^{n_k} W_{k(i,\cdot)}^\top G'_{k(i,\cdot)} \right\rangle_Z \\
&= \left\langle W_k^\top c'_k, W_k^\top G'_k \right\rangle_Z \\
&= W_k^\top \mathcal{G}_k.
\end{aligned}$$

Case (ii). The k -th layer is nonlinear. Prop. 10 proves the correctness. \square

Proposition 12 (Gradient Set w.r.t. Weights and Bias). *The gradients of the set-based loss w.r.t. a weight matrix and a bias vector are*

$$\begin{aligned}
\nabla_{W_k} \mathcal{L}(t, \mathcal{Y}) &= \nabla_{\mathcal{H}_k} \mathcal{L}(t, \mathcal{Y}) \odot \mathcal{H}_{k-1}^\top \\
\nabla_{b_k} \mathcal{L}(t, \mathcal{Y}) &= \nabla_{\mathcal{H}_k} \mathcal{L}(t, \mathcal{Y}) \odot \langle \mathbf{1}, \mathbf{0} \rangle_Z^\top.
\end{aligned}$$

Proof. We rewrite the gradient by applying the chain rule for partial derivatives:

$$\begin{aligned}
\nabla_{W_k} \mathcal{L}(t, \mathcal{Y}) &= \sum_{i=1}^{n_k} c'_{k(i)} \nabla_{W_k} c_{k(i)} \\
&\quad + \sum_{i=1}^{n_k} \sum_{j=1}^q G'_{k(i,j)} \nabla_{W_k} G_{k(i,j)}, \\
\nabla_{b_k} \mathcal{L}(t, \mathcal{Y}) &= \sum_{i=1}^{n_k} c'_{k(i)} \nabla_{b_k} c_{k(i)} \\
&\quad + \sum_{i=1}^{n_k} \sum_{j=1}^q G'_{k(i,j)} \nabla_{b_k} G_{k(i,j)},
\end{aligned}$$

where $G'_k \in \mathbb{R}^{n_k \times q}$. Moreover, we have for dimension $i \in [n_k]$ and generator index $j \in [q]$:

$$\begin{aligned}
\nabla_{W_k} c_{k(i)} &= \nabla_{W_k} (W_{k(i,\cdot)} c_{k-1} + b_{k(i)}) = e_i c_{k-1}^\top, \\
\nabla_{W_k} G_{k(i,j)} &= \nabla_{W_k} (W_{k(i,\cdot)} G_{k-1(\cdot,j)}) = e_i G_{k-1(\cdot,j)}^\top, \\
\nabla_{b_k} c_{k(i)} &= \nabla_{b_k} (W_{k(i,\cdot)} c_{k-1} + b_{k(i)}) = e_i, \\
\nabla_{b_k} G_{k(i,j)} &= \nabla_{b_k} (W_{k(i,\cdot)} G_{k-1(\cdot,j)}) = \mathbf{0},
\end{aligned}$$

where $e_i \in \{0, 1\}^{n_k}$ is the i -th standard basis vector. Thus,

$$\begin{aligned}
\nabla_{W_k} \mathcal{L}(t, \mathcal{Y}) &= c'_k c_{k-1}^\top + G'_k G_{k-1}^\top = \mathcal{G}_k \odot \mathcal{H}_{k-1}^\top, \\
\nabla_{b_k} \mathcal{L}(t, \mathcal{Y}) &= c'_k = \mathcal{G}_k \odot \langle \mathbf{1}, \mathbf{0} \rangle_Z^\top. \quad \square
\end{aligned}$$

Proposition 14. *The zonotopes used in Alg. 2 have at most $q \leq n_0 + \sum_{k \in [\kappa]} n_k$ number of generators. Let $n_{\max} := \max_{k \in [\kappa]} n_{k-1} n_k$ be the maximum size of a weight matrix*

in the neural network. Moreover, Alg. 2 has time complexity $\mathcal{O}(n_{\max} q \kappa)$ w.r.t. n_{\max} , q and the number of layers κ .

Proof. The initial ϵ -perturbation set has n_0 generators (line 1) and every nonlinear layer adds n_k new generators for the approximation errors (Alg. 1). Moreover, there are at most κ nonlinear layers. Thus, in total, there are at most $(n_0 + \sum_{k \in [\kappa]} n_k)$ generators.

Time Complexity: The k -th step of the set-based forward propagation takes time $\mathcal{O}(n_{\max} q)$: The linear map (line 4) as well as the image enclosure (line 6) takes time $\mathcal{O}(n_{k-1} n_k q) = \mathcal{O}(n_{\max} q)$ (Prop. 4 and 13). Hence, the set-based forward propagation (lines 2–6) takes time $\kappa \mathcal{O}(n_{\max} q)$. The gradient of the set-based loss has $(n_\kappa + n_\kappa q)$ entries and the computation of each entry takes constant time; hence, computing the gradient takes time $\mathcal{O}(n_\kappa + n_\kappa q)$. The k -th step of the set-based backpropagation takes at most $\mathcal{O}(n_{k-1} n_k q) = \mathcal{O}(n_{\max} q)$ time: a linear layer computes a linear map (line 11), which takes time $\mathcal{O}(n_{k-1} n_k q)$ (Prop. 4), and the set-based backpropagation of an image enclosure (line 15) takes time $\mathcal{O}(n_{k-1} n_k q)$ (Prop. 10). Hence, the set-based backpropagation (lines 9–15) takes time $\kappa \mathcal{O}(n_{\max} q)$. Updating a weight matrix takes time $\mathcal{O}(n_{k-1} n_k + n_{k-1} n_k q) = \mathcal{O}(n_{\max} q)$ (line 12) and updating a bias vector takes time $\mathcal{O}(n_k) = \mathcal{O}(n_{\max})$ (line 13). There are at most κ linear layers; hence, updating the weight matrix and bias vector of all linear layers takes time $\kappa (\mathcal{O}(n_{\max} q) + \mathcal{O}(n_{\max})) = \kappa \mathcal{O}(n_{\max} q)$. Thus, in total, an iteration of set-based training takes time $3 \kappa \mathcal{O}(n_{\max} q \kappa) = \mathcal{O}(n_{\max} q \kappa)$. \square